Persistence of North Pacific Sea Surface Temperature and Atmospheric Flow Patterns

JEROME NAMIAS, XIAOJUN YUAN* AND DANIEL R. CAYAN

Scripps Institution of Oceanography, University of California, San Diego, La Jolla, California

(Manuscript received 28 September 1987, in final form 7 March 1988)

ABSTRACT

North Pacific monthly sea surface temperature (SST) anomalies are more persistent than a first-order Markov process, often lasting for more than 5 months. Sea surface temperature persistence undergoes an annual cycle that is attributable to the depth of the surface mixed layer and to the annual cycle of forcing. For a given lag, the pattern correlation is minimum when it involves SST during the summer months and maximum when it involves SST during the winter months. Average winter SST anomalies that have exhibited greatest persistence during the last four decades have been negative in the central North Pacific and positive along the West Coast, but antipersistent SST anomalies have not conformed to a repeatable pattern. The atmospheric 700 mb height anomalies associated with high persistence SST cases indicate that strong SST persistence is associated with long-lasting atmospheric anomaly patterns. For highly persistent January SST anomalies, 700 mb anomalies often last from December through February. The high persistence 700 mb anomalies tend to be negative over the east-central North Pacific and positive over North America, with strong teleconnections. This pattern translates to strengthened westerlies over the subtropics and weakened westerlies in middle latitudes across the North Pacific—a zonal wind profile that is nearly opposite to that which appeared in low persistency SST cases.

Over the four decades since 1947, North Pacific SST persistence has undergone substantial multiyear variability, and has increased significantly since the beginning of this record. Related low-frequency fluctuations, as well as linear trends, have occurred in the zonal mean subtropical westerlies across the North Pacific and in related large-scale atmospheric indices, the PNA pattern and the Southern Oscillation Index.

1. Introduction

Anyone who has attempted to make weather forecasts for periods longer than a week soon recognizes that he must deal not with individual days but with statistical ensembles of data. In so doing, he becomes aware that, within periods of a couple of weeks, a month, or even a season, meteorological patterns are autocorrelated. This autocorrelation is usually called persistence, although it frequently manifests itself as a sort of persistent recurrence of patterns with time scales of a week or so (Namias 1954a, 1966). Recurrence over a period of a month or more usually means that a *regime* has set in, which is recognized by repetitions of similar patterns of temperature, precipitation, and particularly, midtropospheric wind. Obviously, if one could anticipate these regimes, he would be able to make more reliable long-range forecasts. While this situation has been recognized by generations of meteorologists, no one has yet found reliable prediction methods. The state of long-range forecasting is therefore still immature, although there has been some modest success in predicting when a weather regime is stable, and even when it is unstable and thus apt to break down.

Is the persistence observed in the atmosphere an intrinsic property of its governing dynamics? It is generally thought that, in addition to internal dynamics, atmospheric anomalies acquire a low-frequency variability that results from interactions with more persistent external elements. Among these external influences is the heating of the atmosphere by the upper ocean. Studies by Namias (1978), van den Dool et al. (1986) and Van den Dool and Chervin (1986) show that midlatitude surface air temperature anomalies over land are more persistent near large bodies of water than those in continental interiors. To better identify the associated circulation, a major theme of this study is a comparison of atmospheric behavior during those episodes when the ocean's persistence is greatest with its behavior during those episodes when persistence is least. This approach complements a previous study of the persistence of American atmospheric flow patterns over the North American sector (Namias 1986), which presented evidence that certain patterns tend to persist while others tend to be unstable.

The ocean considered here is the extratropical North Pacific, represented by the sea surface temperature

* Permanent affiliation: National Research Center for Marine Environment Forecast, Beijing, China.

Corresponding author address: Dr. Jerome Namias, Scripps Institution of Oceanography, A-024, University of California San Diego, La Jolla, CA 92093.

(SST) field. Many previous studies have demonstrated the connection between North Pacific SST and the anomalous atmospheric circulation overlying and downstream (e.g., Namias 1975, 1983; Davis 1978; Frankignoul 1985). Because of the close interrelationship between SST patterns and upper-level flow patterns over the North Pacific and North America, a study involving the persistence of North Pacific sea surface temperatures (SST values) can throw further light on prolonged air–sea interaction regimes as well as aid long-range forecasting. Observations show episodes with impressive persistence of SST anomalies over several months. An example is a sequence of maps for the period January–June 1987 (Fig. 1), which show negative SST anomalies in the central North Pacific and positive SST anomalies along the eastern boundary. This same configuration remained for at least 6 months before it changed.

To explore the persistence of SST in the North Pacific, we compare high and low persistence SST patterns. We then examine the accompanying atmospheric flow patterns through the use of monthly 700 mb height anomalies and associated zonal winds. Finally, we describe some long-period swings in persistence and relate them to atmospheric and oceanic regimes.

2. Data sources and data analyses

The basic datasets used in this study consist of monthly and seasonal mean North Pacific sea surface temperature (SST) and Northern Hemisphere 700 mb heights for the period 1947–87. The SST data are based

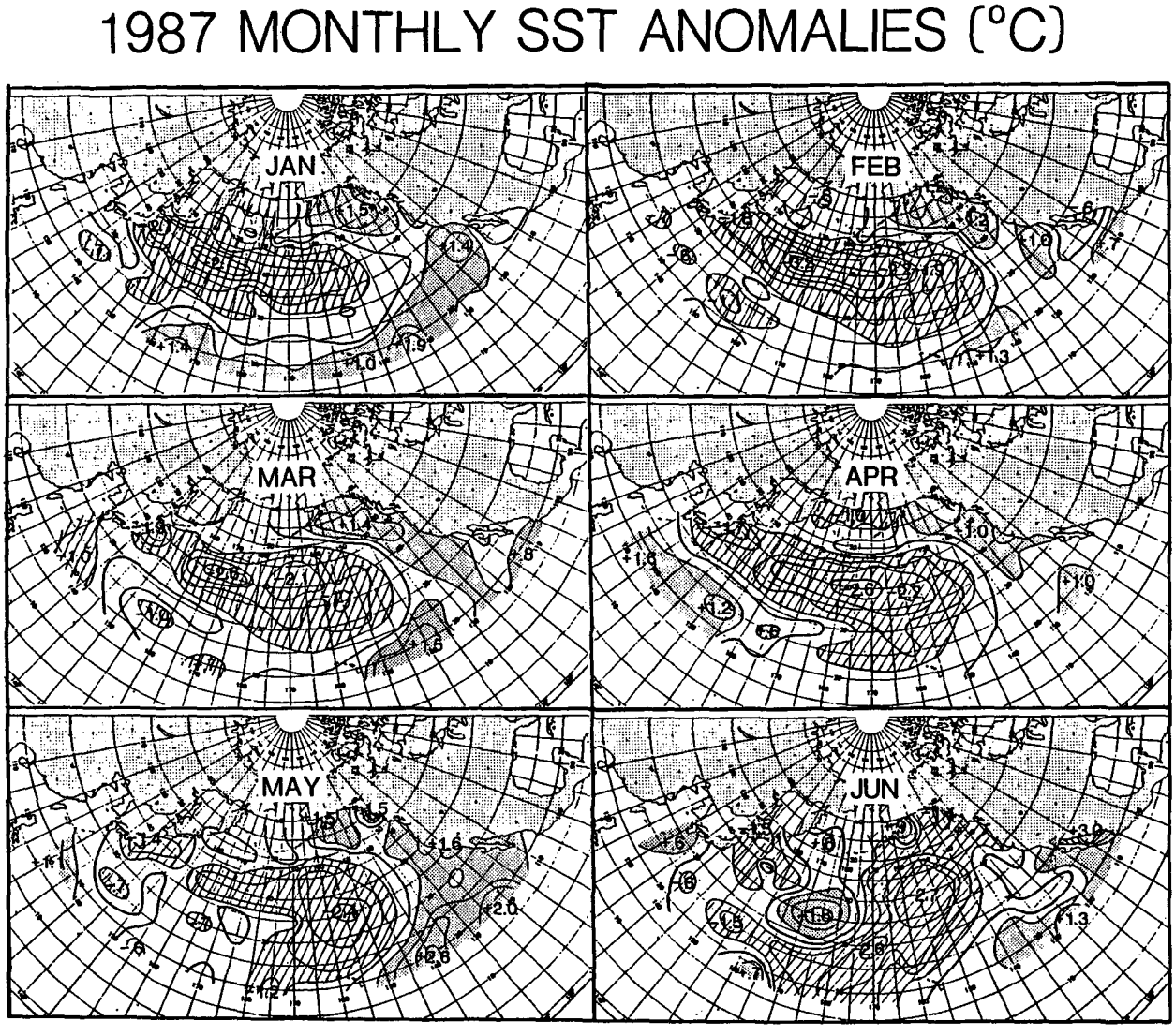

FIG. 1. A good example of persistent monthly SST anomalies, January–June 1987. Anomalies (°C) calculated on the basis of 1947–66 long-term monthly means.

on ship observations originally computed in the form of monthly averages from a 2° latitude–longitude grid. Details of the SST data up to the 1970s were described by Namias (1970, 1979) and Davis (1976). The 700 mb height values were taken from monthly averages supplied by the Long Range Prediction Group of the National Meteorological Center (NMC) for a 5° latitude–longitude "diamond grid" over the Northern Hemisphere from 15° or 20°N to 80°N. Both the SST and 700 mb datasets were processed into a 5° latitude–longitude grid covering 20° to 60°N and 130°E to 110°W of the North Pacific.

For the North Pacific SST and 700 mb height (Namias 1979), anomalies based on a 20-year mean (1947–66) were readily available, and it is these anomalies that are used in the analyses that follow. While the choice of base period for the long-term means affects the numerical values of the anomalies and the pattern correlations presented here, selected analyses of anomalies based on the entire dataset showed results that did not materially change from those using the shorter base period. Thus, it was decided to use the 20-yr base period for ease of computation because anomalies from this time base are already available at the Climate Research Group. It is important to note that in the analyses presented, the linear trend was not removed from the anomaly time series, thus retaining the low-frequency contribution to the persistence, which plays an important role as pointed out in section 6.

The number of spatial samples for the North Pacific 700 mb grid is 225 while for the SST field, it is only about 160 due to the fact that grid points occur close to land and some are poorly represented because of missing data. Since there is considerable spatial correlation between the 700 mb and SST anomalies, the number of independent samples is far less than the number of grid points. Following Horel (1985), the number of independent spatial samples can be estimated from the standard deviation of the z-transformed pattern correlations over the record. Assuming the z-transformed pattern correlation is normally distributed (Panofsky and Brier 1958), its standard deviation is given as $1/(Ne-4)^{1/2}$, where Ne is the effective number of independent samples (or degrees of freedom). Equating this to the standard deviation of the ensemble of pattern correlations for all initial months over lags of 1 to 12 months in the sample, Ne is approximately equal to 8 and 16 for the 700 mb height and SST anomalies, respectively. The larger spatial correlation (fewer degrees of freedom) of 700 mb height anomalies relative to the SST anomalies has also been noted by Davis (1976).

The variance of the SST and 700 mb height changes considerably over the North Pacific grid. The SST standard deviation ranges by a factor of 3–5, and the maxima along 30°N is especially large in the western boundary region east of Japan. The standard deviation of 700 mb height ranges by a factor of 5–7, with a well-known maximum in the region south of the Aleutians, eastward to the Gulf of Alaska. These variance maxima are important because they have great influence on the computation of the pattern correlations presented.

3. SST Anomaly patterns for high and low persistence

To measure the skill of persistence, pattern correlations of observed SST from a given initial month, with SST observed at a lag of 1 to 12 months later, were made for every forecast month. The pattern correlation is defined as

$$\rho = \frac{\sum_x (s_0 - \bar{s}_0)(s_1 - \bar{s}_1)}{[\sum_x (s_0 - \bar{s}_0)^2 \sum_x (s_1 - \bar{s}_1)^2]^{1/2}}$$

where ρ is the correlation coefficient; s_0, the SST anomaly of a particular grid point for month 0; $\bar{s}_0$, the mean anomaly over the entire grid for month 0; s_1, the SST anomaly of a particular grid point for month 1; $\bar{s}_1$, the mean anomaly over the entire grid for month 1; and $\sum_x$ represents the sum over the entire North Pacific grid. Pattern correlations of the anomalies of SST for 1 to 12 months lag were calculated for available pairs of maps over the 1947–87 period for all initial months.

To evaluate average persistence over the entire record, we calculated the long-term mean of the pattern correlation at each of 12 monthly time lags, as shown in Table 1. In comparison to various members of the atmospheric circulation, whose pattern correlation of monthly averages falls below 0.3 after just one month's lag (Namias 1986; Van den Dool and Chervin 1986; see also Table 3), the SST pattern correlation remains above 0.3 until lags of 3 to 5 months. For the purposes of this study, which aims to characterize the overall SST persistence out to several months for a given period, the average persistence over various monthly lags was examined. Averages of the pattern correlation over lags 1–3, 1–6, 1–9 and 1–12 from the initial months of January, April, July and October are shown in Fig. 2. The averaging scheme over these lags is illustrated in Table 2. The SST pattern correlations with lags out to 3 months have the most persistent patterns initiating from January, while pattern correlations are lower starting from April and July. The 6-month persistence graphs tend to be similar in shape to those of the first 3 months but with lower average correlations.

Assuming that the pattern correlation is normally distributed, the significance of differences in the mean pattern correlation can be estimated from its standard deviation, given by $1/(N-2)^{1/2}$, where N is the number of independent observations. In this case, there are about 16 spatial samples estimated in the grid and 40 samples averaged together in the record, assuming that each year's data is independent from the last; this gives a total of 640 independent samples in the mean to yield a standard deviation of approximately 0.04.

TABLE 1. Mean North Pacific SST pattern correlation (1947–85).

Initial month	Lag (months)												
	0	1	2	3	4	5	6	7	8	9	10	11	12
1	1.00	0.62	0.55	0.38	0.31	0.22	0.20	0.14	0.10	0.11	0.12	0.15	0.19
2	1.00	0.60	0.47	0.37	0.24	0.22	0.14	0.10	0.13	0.15	0.18	0.22	0.18
3	1.00	0.57	0.46	0.32	0.28	0.20	0.16	0.18	0.21	0.24	0.25	0.22	0.20
4	1.00	0.55	0.37	0.29	0.19	0.16	0.20	0.23	0.24	0.22	0.17	0.17	0.14
5	1.00	0.51	0.38	0.28	0.20	0.24	0.28	0.25	0.23	0.20	0.20	0.17	0.18
6	1.00	0.52	0.32	0.24	0.23	0.24	0.22	0.20	0.20	0.19	0.17	0.17	0.16
7	1.00	0.51	0.35	0.28	0.21	0.19	0.17	0.17	0.13	0.15	0.16	0.15	0.11
8	1.00	0.51	0.32	0.23	0.18	0.14	0.16	0.16	0.12	0.14	0.12	0.11	0.11
9	1.00	0.50	0.30	0.23	0.16	0.14	0.15	0.11	0.10	0.12	0.16	0.13	0.14
10	1.00	0.56	0.40	0.28	0.29	0.25	0.17	0.17	0.15	0.15	0.11	0.09	0.15
11	1.00	0.55	0.39	0.33	0.32	0.23	0.20	0.16	0.12	0.06	0.04	0.06	0.05
12	1.00	0.54	0.49	0.42	0.29	0.25	0.19	0.15	0.08	0.06	0.08	0.11	0.15

Like atmospheric circulation, the persistence of SST is greatest in winter, with a maximum in January. However, unlike the atmospheric circulation, which has a secondary maxima in persistence in summer (see van den Dool 1983; Namias 1986), SST persistence is lowest in summer. Differences in the mean pattern correlation between summer (June–September) leading months and the cool season range between 0.10 and ~0.20, which would be highly significant by the standard deviation measure above. Following Namias and Born (1970), who studied the annual cycle in SST persistence in a shorter 1947–66 dataset, the changes over the years in the strength of SST persistence are due largely to the vertical profile of density in the upper ocean and the annual cycle of atmospheric forcing. The upper mixed layer is thickest in late winter and thinnest in summer. In winter, the large, deep thermal anomaly reservoir is hard to change; in summer, thermal stratification makes a strong seasonal thermocline and a thin lense of near-surface water, which can undergo considerable change with heating or vertical mixing. One exercise that demonstrates the strength and annual cycle of SST persistence is to compare the pattern correlations with correlations that would occur if the anomalies were governed by a first-order Markov process, $SST_{m+1} = \rho SST_m + n_{m+1}$, where ρ is the one-month lag correlation of SST, n is the part of SST in month $m + 1$ that is uncorrelated with SST in month m_0. The difference between the mean monthly lag pattern correlations of Table 1 and those from the Markov process are illustrated in Fig. 3, giving contours of the correlation differences at 0.05 intervals. Using the standard deviation of the mean pattern correlation calculated above as a guide, differences between the mean pattern correlation and the Markov process in excess of about 0.04 would be significant. To emphasize the strongest features, differences of 0.20 and greater are shaded in Fig. 3. These differences are for all lags (2 through 12) greater than zero, with maxima for winter correlations leading to spring months at lags of 3 to 5 months, and also for correlations leading to winter from the previous winter at lags of 6 to 11 months. There is a distinct minimum in these differences for correlations from summer and leading to summer. This supports the idea that the thermal memory of the extratropical upper ocean is usually established in winter by vigorous storm activity, remains strong into spring when the mixed layer is still present but when vigorous atmospheric forcing is declining, is weakest in summer because of a thin stable layer, and recovers (albeit at a low level) in winter as the surface layer remixes with the subsurface features established during the previous winter.

TABLE 2. Average monthly SST persistence over 3, 6 and 9 month lags starting from January.

Following months										
2	3	4	5	6	7	8	9	10	11	12
3-mo. avg.										
6-mo.avg.										
9-mo. avg.										

The strength of the winter mean SST pattern correlations and a visual inspection of many graphs and maps indicate that much can be learned from the macroscale conditions associated with winter North Pacific SST persistence. Lag correlations from January are largest and perhaps contain the most significant results. Thus, in the remainder of this paper, analyses are confined to those associated with SST persistence from January forward.

As an index of the January SST persistence, the 1 to 6 lag average pattern correlations from January (see Table 2) were used to diagnose associated SST and 700 mb anomaly patterns. Six-month average persistence values were ranked and divided into quartiles covering

TABLE 3. Mean North Pacific 700 mb height pattern correlation (1947–85).

Initial month	Lag (months)												
	0	1	2	3	4	5	6	7	8	9	10	11	12
1	1.00	0.19	0.06	0.02	−0.02	0.03	0.06	0.08	−0.08	−0.01	−0.12	0.04	0.02
2	1.00	0.15	0.15	−0.01	0.02	0.04	0.05	−0.06	0.03	0.07	0.10	0.07	0.05
3	1.00	0.19	0.21	0.10	0.09	0.10	0.07	0.01	0.06	−0.03	−0.02	0.02	0.04
4	1.00	0.18	0.09	0.09	−0.02	0.03	0.03	0.14	0.04	−0.05	0.07	0.10	0.07
5	1.00	0.17	0.08	0.01	0.07	0.04	0.01	−0.08	−0.05	0.06	−0.03	0.03	0.03
6	1.00	0.09	0.01	0.03	−0.02	−0.01	0.03	0.03	0.01	0.08	0.14	0.10	0.06
7	1.00	0.14	0.03	0.06	−0.03	0.09	0.02	0.10	0.09	0.08	0.09	0.08	0.06
8	1.00	0.17	0.05	0.05	−0.09	−0.08	0.07	−0.01	0.05	0.05	0.12	0.09	0.01
9	1.00	0.02	0.02	0.04	−0.12	0.09	−0.06	0.11	−0.02	0.05	0.17	0.09	0.09
10	1.00	0.19	0.04	0.04	0.05	−0.01	−0.02	0.00	−0.03	−0.03	0.02	−0.04	0.07
11	1.00	0.11	−0.01	0.09	0.07	0.06	0.01	0.08	0.02	−0.08	−0.04	−0.03	0.08
12	1.00	0.26	0.17	0.00	−0.03	−0.05	−0.02	0.02	0.10	−0.07	0.13	0.14	0.04

the 33-yr subset from 1950 to 1982. This provided a picture of SST anomaly patterns that are highly persistent (upper quartile) as well as least persistent (lowest quartile). High quartile Januaries (in order of strength of SST persistence) were 1981, 1958, 1956, 1961, 1978, 1959, 1969 and 1980. The low quartile (from lowest upwards) consists of the Januaries of 1955, 1951, 1967, 1973, 1964, 1954, 1966 and 1953. The mean of the 1 to 6 lag average pattern correlations was 0.57 for the high persistence cases and 0.14 for the low persistence cases. Composite SST anomaly maps of the high and low quartile January cases were formed, as shown in

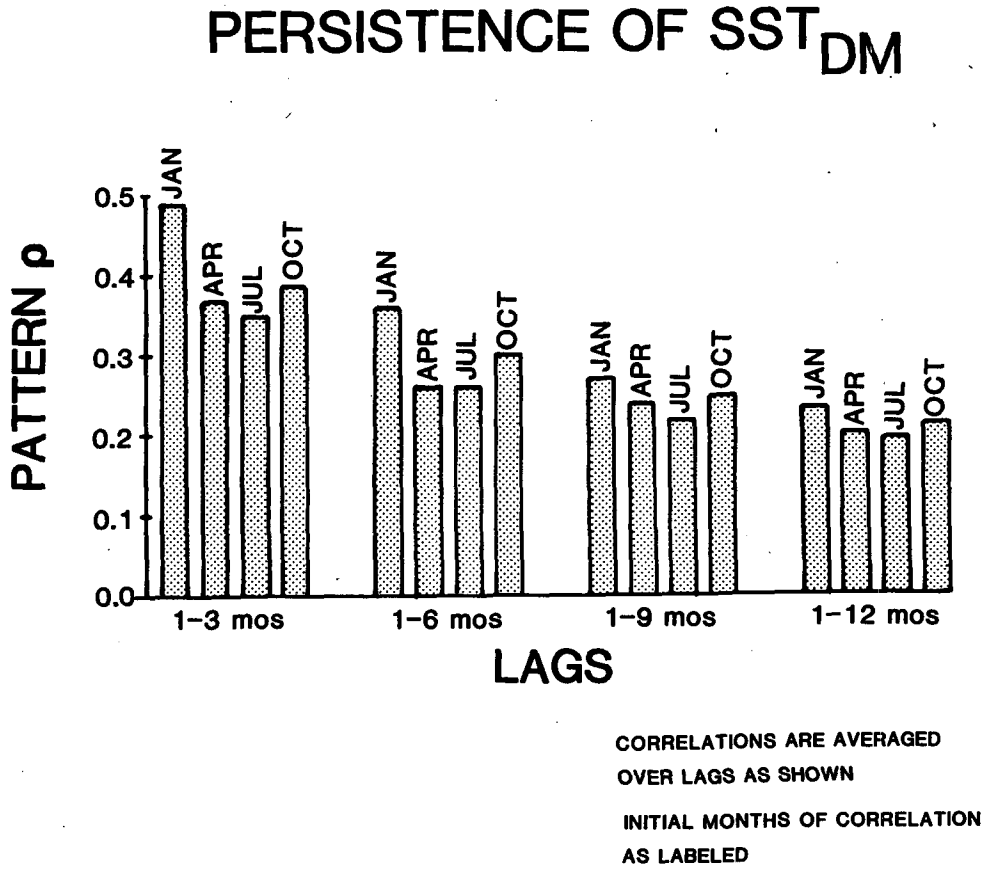

FIG. 2. Mean pattern correlations of North Pacific SST anomalies averaged over 3, 6, 9 and 12 months for period 1950–82. Pattern correlations shown for four initial months (January, April, July, and December).

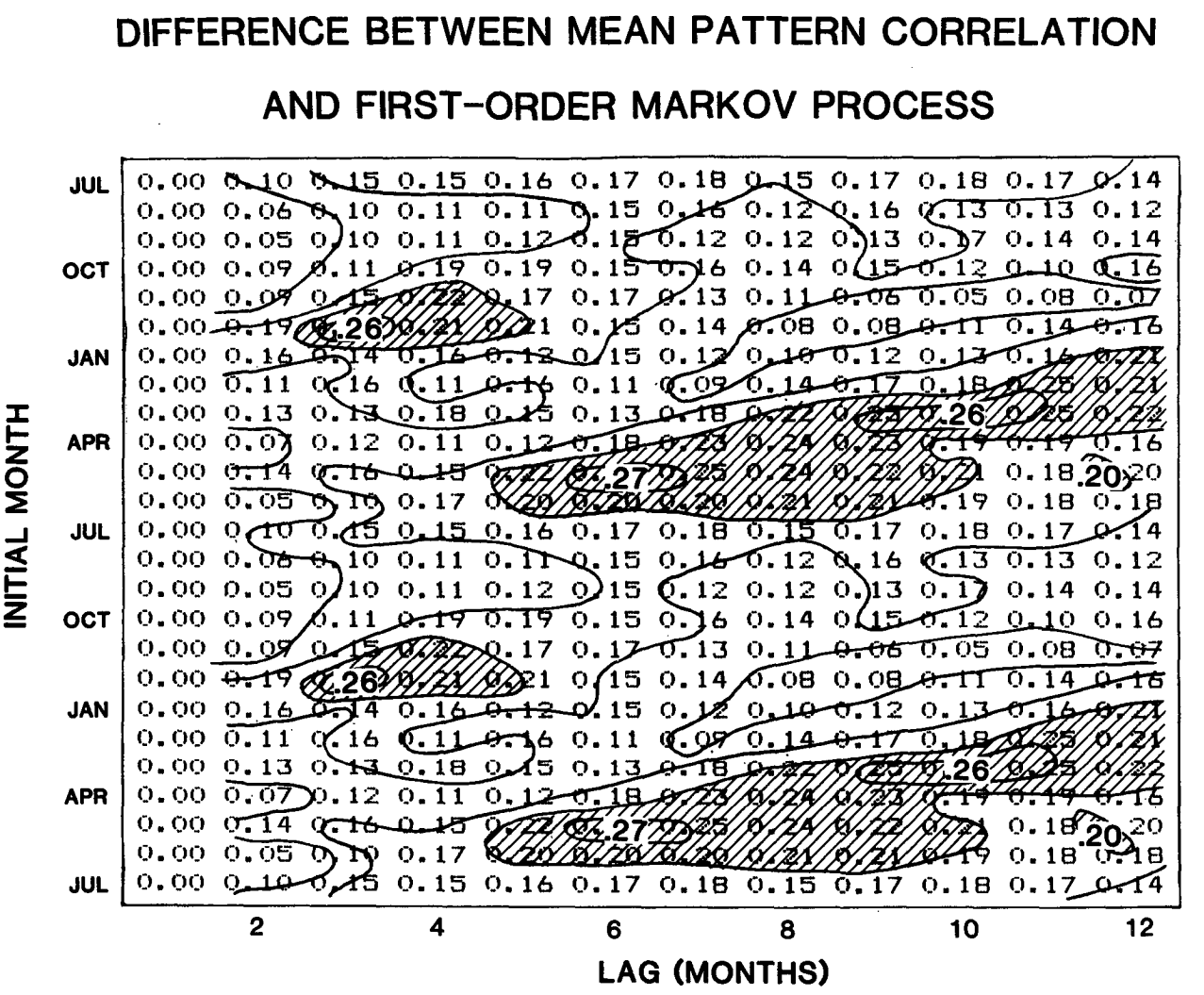

FIG. 3. Differences between average monthly lag pattern correlation and a first-order Markov process having the same lag-1 correlation. Pattern correlations based on anomalies from 1947–66 long-term monthly mean. Averages over 1947–87.

Figs. 4 and 5, and areas that exceed the 5% level of significance were delineated with appropriate shading. For the composite anomalies shown here and the ones presented in section 4, significance was calculated by a two-tailed *t*-test. To exceed the 5% level of significance, the composite anomaly at any grid point divided by its standard deviation/$\sqrt{8}$ must exceed 2.02 for this particular data series, under the assumption that each January is an independent sample. Regions with anomalies meeting this criteria are shaded on the composite maps.

The composite SST anomaly pattern for low persistence (Fig. 5) is weak, indicating a lack of consistency. On the other hand, the composite SST anomaly pattern for the high persistent cases (Fig. 4) is fairly strong—particularly in the eastern half of the North Pacific where the strong negative anomaly of SST in the initial month (January) and the equally strong positive anomaly to its east appear. Both of these features are significant at the 5% level. The gradient between these two anomalous pools of surface water is noteworthy because this type of pattern has been described in many reports and has been invoked to explain the atmospheric baroclinity induced by the SST gradient and its associated heat fluxes (Namias 1972; Harnack and Broccoli 1979). It is suspected that this gradient would strengthen fronts and enhance cyclone development, which would then feed back to enhance the oceanic contrast and thus perpetuate the pattern established in January.

In addition to the connection between SST persistence and the spatial configuration of the anomalies, it is of interest to determine if the magnitude of the anomalies has an influence on their ability to persist. Visual inspection of a sequence of monthly SST maps, such as those in Fig. 1, suggests that patterns with large

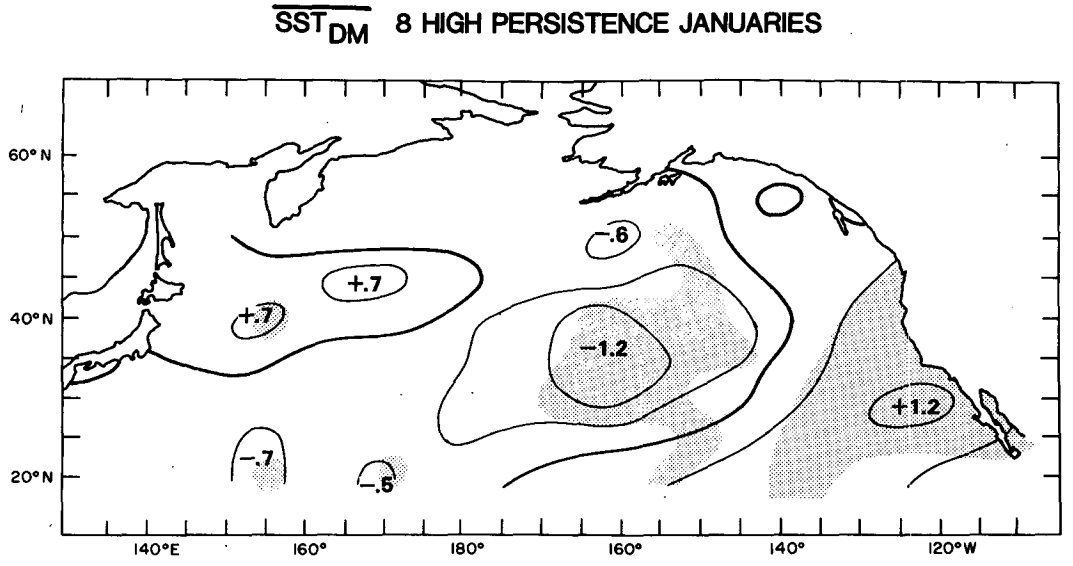

FIG. 4. Mean SST anomaly pattern for the *highest* quartile of SST persistence values from January out to 6 months. Lines are for each 0.5°C and shaded areas exceed the 5% level of significance.

anomalies often persist longest. This is to be expected since the thermal anomaly associated with large SST anomalies would also be large if the upper mixed layer is deep. Mathematically, this is easily seen if the SST anomaly is represented by a first-order Markov process, as discussed above. Under this model, the sign of an anomaly is less likely to change as it becomes larger in magnitude. This general notion is supported by the correlation of the basin average SST anomaly magnitude versus the SST persistence (given by the 1 to 6 lag average pattern correlation). This correlation is +0.47 for January SST leading cases; similar results were obtained from the same calculation for other initial months, ranging from about 0.4 to 0.6.

In section 4, SST pattern persistence is further investigated by constructing the anomalous atmospheric circulation associated with high/low SST persistence. Larger SST anomalies tend to last longer, and the longest lived anomalies remain strong for several months. Two primary questions are How were the SST anomalies generated? and Why do they assume a particular pattern? The development of high/low persistence SST

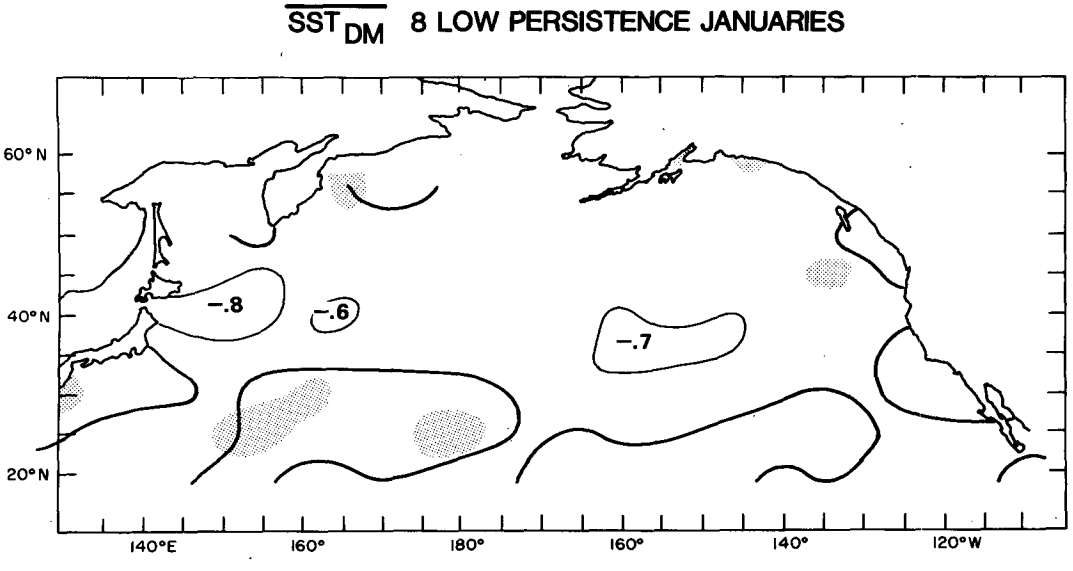

FIG. 5. As in Fig. 4, except for the *lowest* quartile of persistence cases from January forward to 6 months.

anomaly patterns has been examined by studying the circulation anomalies leading up to and following the high/low persistence January SST patterns.

4. The 700 mb patterns associated with high and low SST persistence

The January 700 mb composites associated with highest and lowest cases of January SST persistence are shown in the middle panels of Figs. 6 and 7, where the shaded area indicates areas in excess of the 5% level of significance. These charts exhibit broad-scale and significant anomaly patterns, which result in large-scale air–sea interactions, as represented by their companion SST anomalies in Figs. 4 and 5. Corresponding to the high SST persistence cases, there is a negative 700 mb height anomaly center over the eastern Pacific in January (Fig. 6), which is well related to the high persistence SST anomaly pattern in Fig. 4—cool surface water in the central East Pacific and warm water along the West Coast. In fact, the high persistence composites in Figs. 4 and 6 are favored patterns of covariability and closely resemble one phase of the first empirical orthogonal functions (EOFs) of North Pacific SST and 700 mb shown in Fig. 8. The physical connection between this 700 mb anomaly distribution and SST involves southerly air flow components to the east of the negative 700 mb height anomaly, and northerly components to its west. Negative height anomalies are usually associated with increased upwelling. A strengthened north–south gradient indicates increased westerly winds with large sensible and latent heat exchanges to the south of the 700 mb height anomaly center.

In section 3, which showed a strong high persistence SST distribution and indicated that large SST anomalies persist longer than small ones, it was implied that

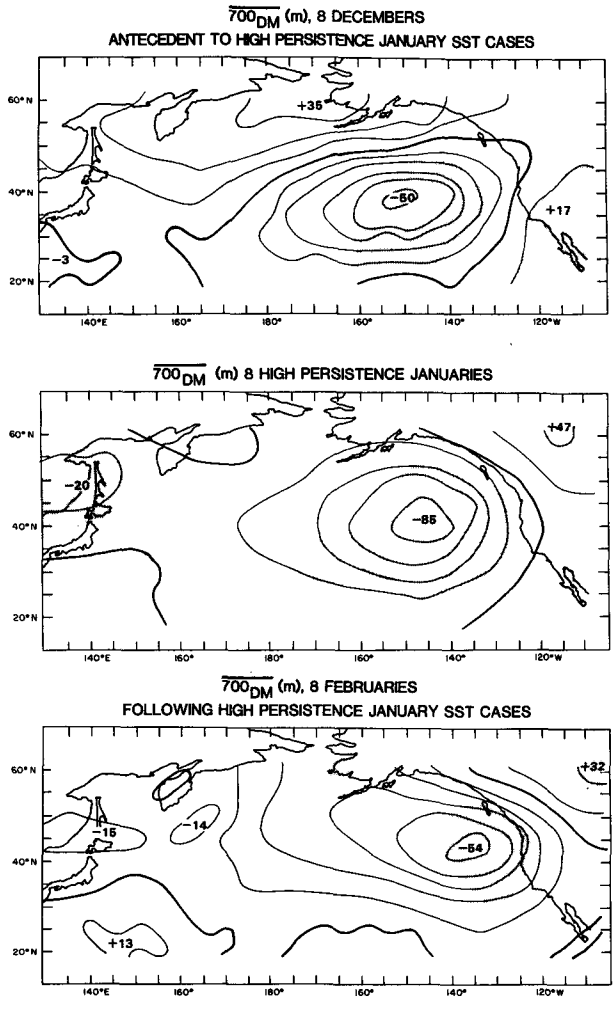

FIG. 6. Mean 700 mb anomalies for the *highest* quartile of January SST pattern persistence index. Composites for antecedent Decembers, Januaries, and Februaries shown in upper, middle, and lower panels, respectively. Compare with Fig. 4.

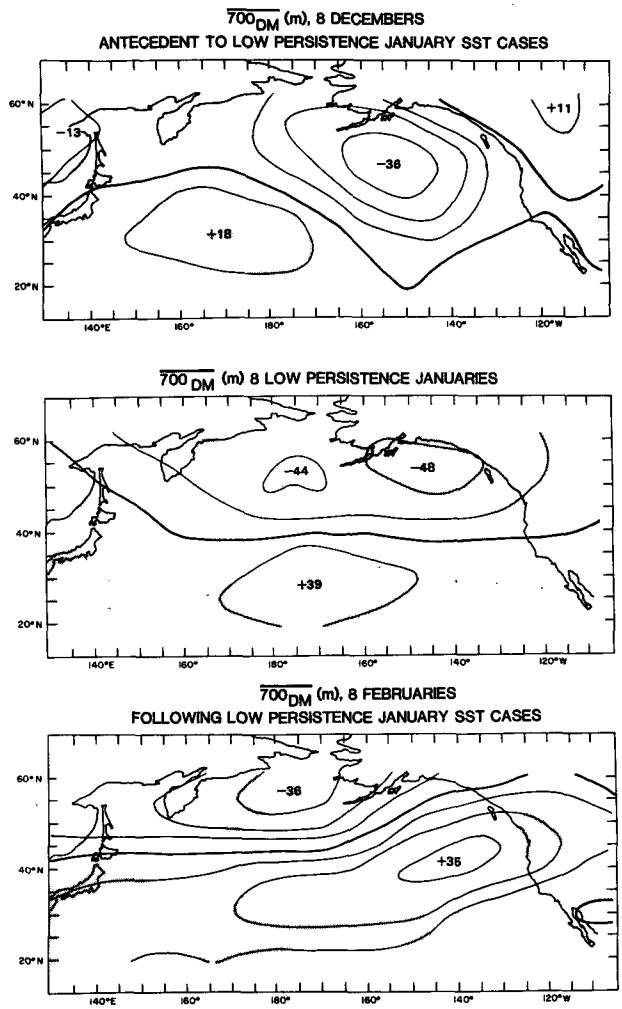

FIG. 7. As in Fig. 6 except for *lowest* quartile of cases. Compare with Fig. 5.

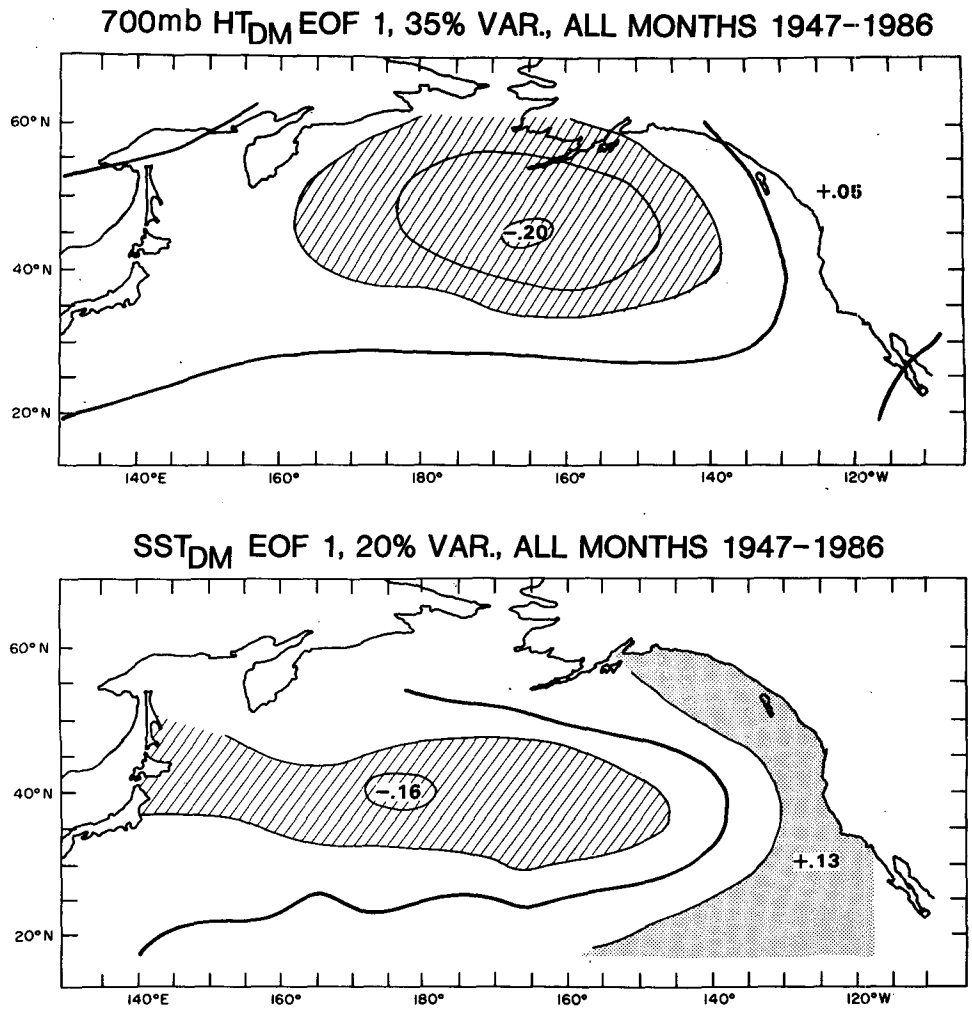

FIG. 8. First EOF of North Pacific monthly 700 mb height (upper) and SST (lower) anomalies. Based on all months, 1947–87. These account for about 35% and 20% of the 700 mb height and SST anomaly variance, respectively.

there should have been an evolution of the North Pacific SST anomaly over antecedent months that led to the resultant strong January pattern. To see the atmospheric component of forcing associated with this development, composites of the 700 mb height anomalies for the eight Decembers and Novembers prior to the high persistence Januaries were constructed. The November composite anomalies were weak, but those for December, shown in the upper panel of Fig. 6, were strong and similar to the January composite. Further, the 700 mb height pattern that took hold in December and January persisted into February, as shown in the lower panel of Fig. 6. All three composites feature large and significant negative heights in the eastern North Pacific, with a tendency for significant positive height anomalies over western North America west of Oregon and California.

The analogous sequence of 700 mb anomaly composites associated with low January SST persistence is not nearly as consistent as it is for the high persistence composites. Although there are large anomaly magnitudes on each of the three maps, the pattern changes remarkably among the three, as shown in Fig. 7. There is a fair resemblence between December and January: both have negative height anomalies in the Gulf of Alaska, and positive anomalies in the subtropical North Pacific. Statistical regressions (not shown) and synoptic experience show that this early winter circulation is consistent with the SST pattern of negative anomalies in the central North Pacific and positive anomalies in the subtropics (Fig. 5). However, a weakened change appears in the February composite, where positive anomalies replace negative height anomalies in the eastern North Pacific (lower panel, Fig. 7). Thus, in December and January, a circulation with frequent storminess across the middle latitude eastern and central North Pacific gives way to a different regime in February indicated by the positive height anomalies,

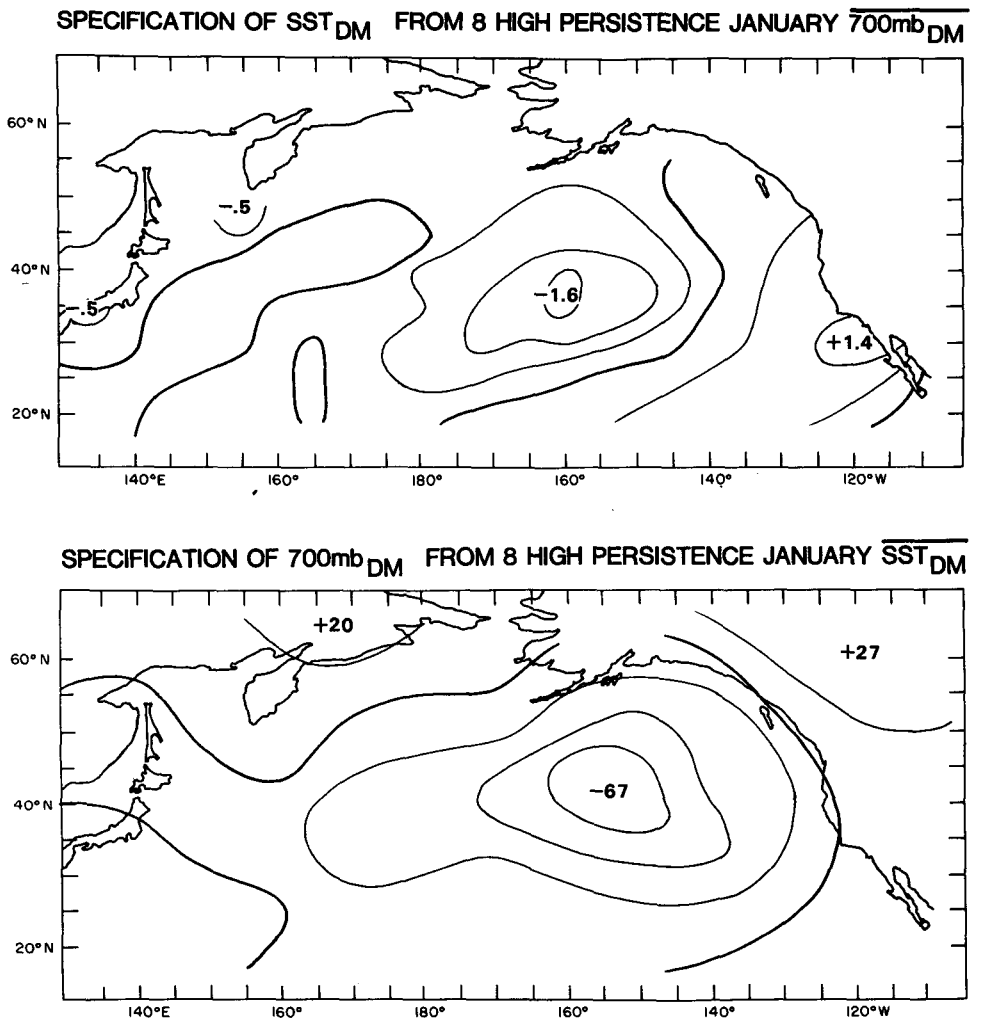

FIG. 9. Above: specification (from linear regression) of SST anomalies from composite 700 mb anomalies corresponding to highest quartile SST persistence cases in Fig. 6. Below: specification of 700 mb anomalies from mean of *highest* quartile of cases of SST anomaly shown in Fig. 4.

with storms tracks diverted north into the Aleutians. This turnabout in the atmospheric circulation is consistent with the low SST persistence that was used to select these cases.

These physical factors can be statistically represented by multiple regressions (specifications) of SST anomalies from 700 mb anomalies, and vice versa, displayed in Fig. 9 for the high persistence cases and in Fig. 10 for the low persistence cases. These specifications are based on stepwise multiple regression (screening) techniques (Namias and Born 1972), similar to those used for United States temperature anomalies (Klein 1985). The correspondence of these specifications with the observed composite anomalies for high persistence (Figs. 4 and 6) and low persistence (Figs. 5 and 7) is good.

High persistence SST cases seem to be associated with major atmospheric modes of variability. The composite pattern of 700 mb height anomalies for the high persistence January SST extends well beyond the North Pacific basin (Fig. 11), with large centers in the eastern North Pacific at about 40°N, 150°W, over central Canada at about 60°N, 100°W, and along the Atlantic seaboard at 35°N, 75°W. This composite is in excellent agreement with the statistically constructed 700 mb teleconnections for winter from the entire dataset. Teleconnection maps (not shown, but see, e.g., Namias 1981) from any of the three above centers are nearly identical in pattern to the composite, indicating the internal consistency and stability of the large-scale circulation. Furthermore, this anomaly configuration resembles the positive phase of the well-known Pacific/North American (PNA) pattern (Horel and Wallace 1981). This pattern occurs frequently (Barnston and Livezey 1987; Davis 1976), often during El Niño (Dickson and Livezey 1984), but also under other cir-

cumstances (Douglas et al. 1982; Palmer 1987). This pattern is also associated with the high month-to-month persistence of the 700 mb height field—both preceding and during El Niño (Namias 1986). Finally, this pattern may be self-perpetuating. The gradients of SST in the eastern Pacific provide atmospheric baroclinicity that encourages the development and movement of fronts and cyclones, which, in turn, help regenerate the mean pattern shown (Harnack and Broccoli 1979). Because the climatological west-to-east mean ocean currents (Meehl 1982) in the region of the strongest SST anomaly gradient are small, it is clear that advection of SST anomalies by mean surface ocean currents (not shown) would be weak and thus conducive to maintaining the existing thermal pattern of the composite SST high persistence pattern (Fig. 4).

5. Relationship of SST persistence to zonal wind speeds

The 700 mb patterns (Figs. 6 and 7) corresponding to extreme SST persistence exhibit large anomalies that occupy a significant fraction of the North Pacific basin, which implies that there are substantial perturbations in the zonal average wind across the North Pacific. Previous studies that have dealt with the stability of global atmospheric circulation have related it to the index cycle (e.g., Rex 1950; Namias 1953) or the zonal/meridional character of the flow (van den Dool 1983; Roads and Barnett 1984; Horel 1985; and Mo and Ghil 1987). Recently, Namias (1986) found that the persistence of pattern over the Pacific–North America–North Atlantic sector was closely related to the persis-

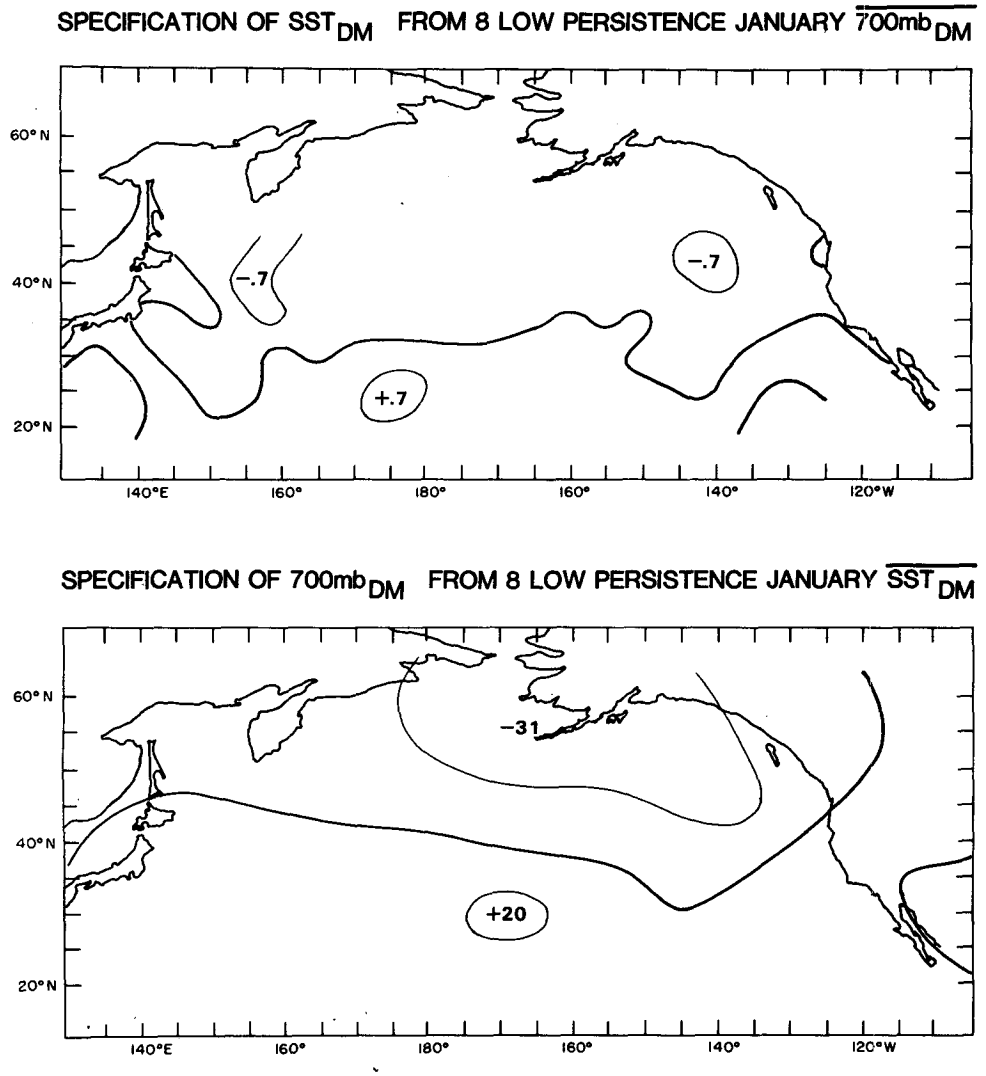

FIG. 10. Above: specification (from linear regression) of SST anomalies from composite January 700 mb anomalies corresponding to lowest quartile of SST persistence cases in Fig. 7. Below: specification of 700 mb anomalies from composite of *lowest* quartile of SST anomaly cases in Fig. 5.

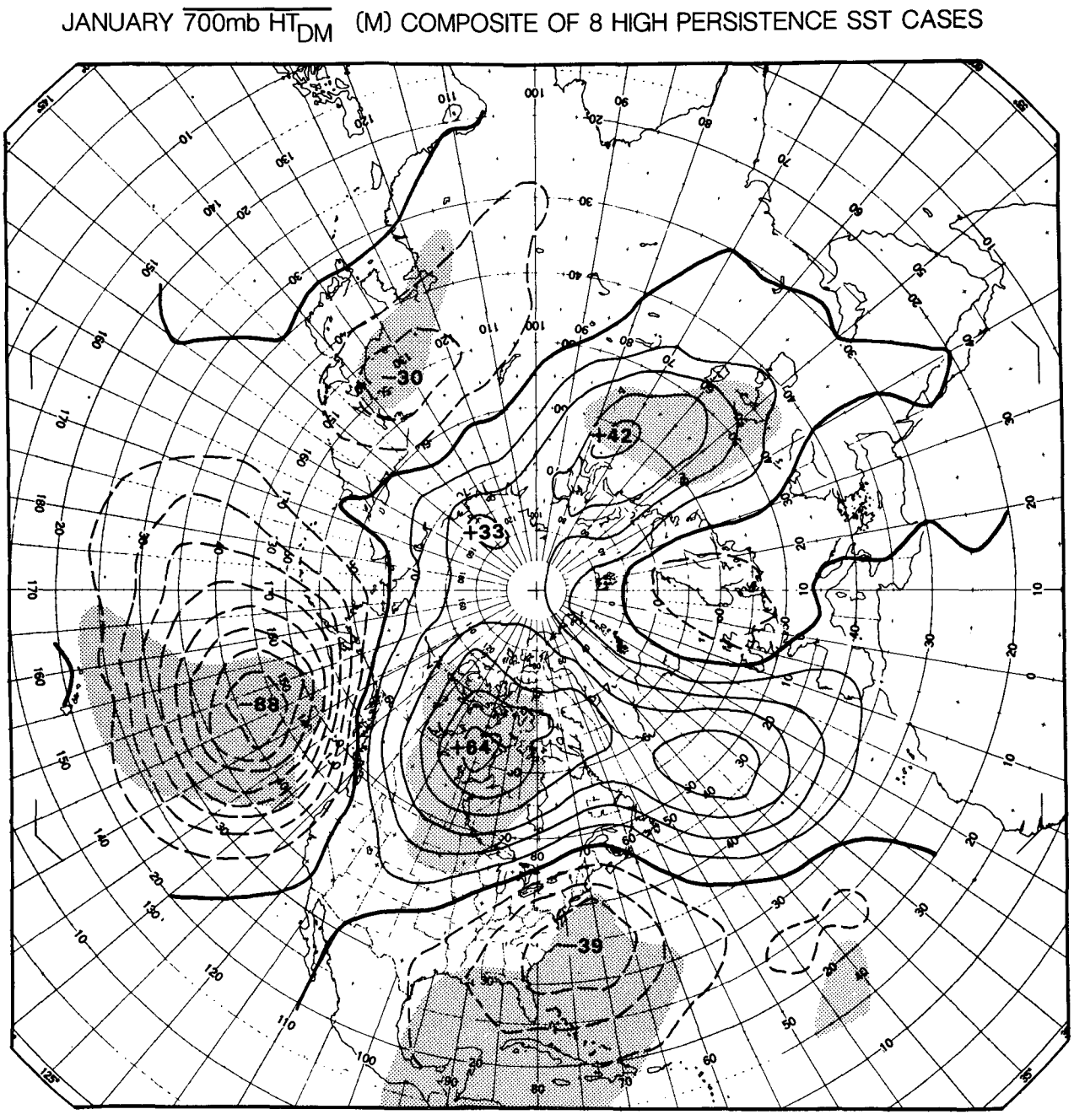

FIG. 11. Composite of January 700 mb height anomalies (m) for high persistent January SST cases, as in Fig. 6, middle, but for entire Northern Hemisphere.

tence of the zonal wind in that sector. Narrowing our scope to the North Pacific, How do these relationships hold up, and what is the relation between zonal wind and SST persistence?

To evaluate the impact of these anomalies, composite 700 mb North Pacific zonal wind anomalies for the January high and low persistence quartiles are plotted (Fig. 12, upper/lower). Besides the January composite profiles, composites for the Novembers and Decembers antecedent to January, and the Februaries, Marches, and Aprils subsequent, are shown in Fig. 12. These are geostrophic winds, $\bar{u} = -(1/f)(\Delta\bar{\Phi}_{700}/\Delta y)$, where $\bar{u}$ is the zonal average east–west geostrophic wind, f the Coriolis parameter, Δy distance along the meridian between two grid points, and $\Delta\bar{\Phi}_{700}$ the difference in geopotential, averaged across the North Pacific domain. In addition to the zonal wind anomalies, the mean speeds, shown in Fig. 13 for the high persis-

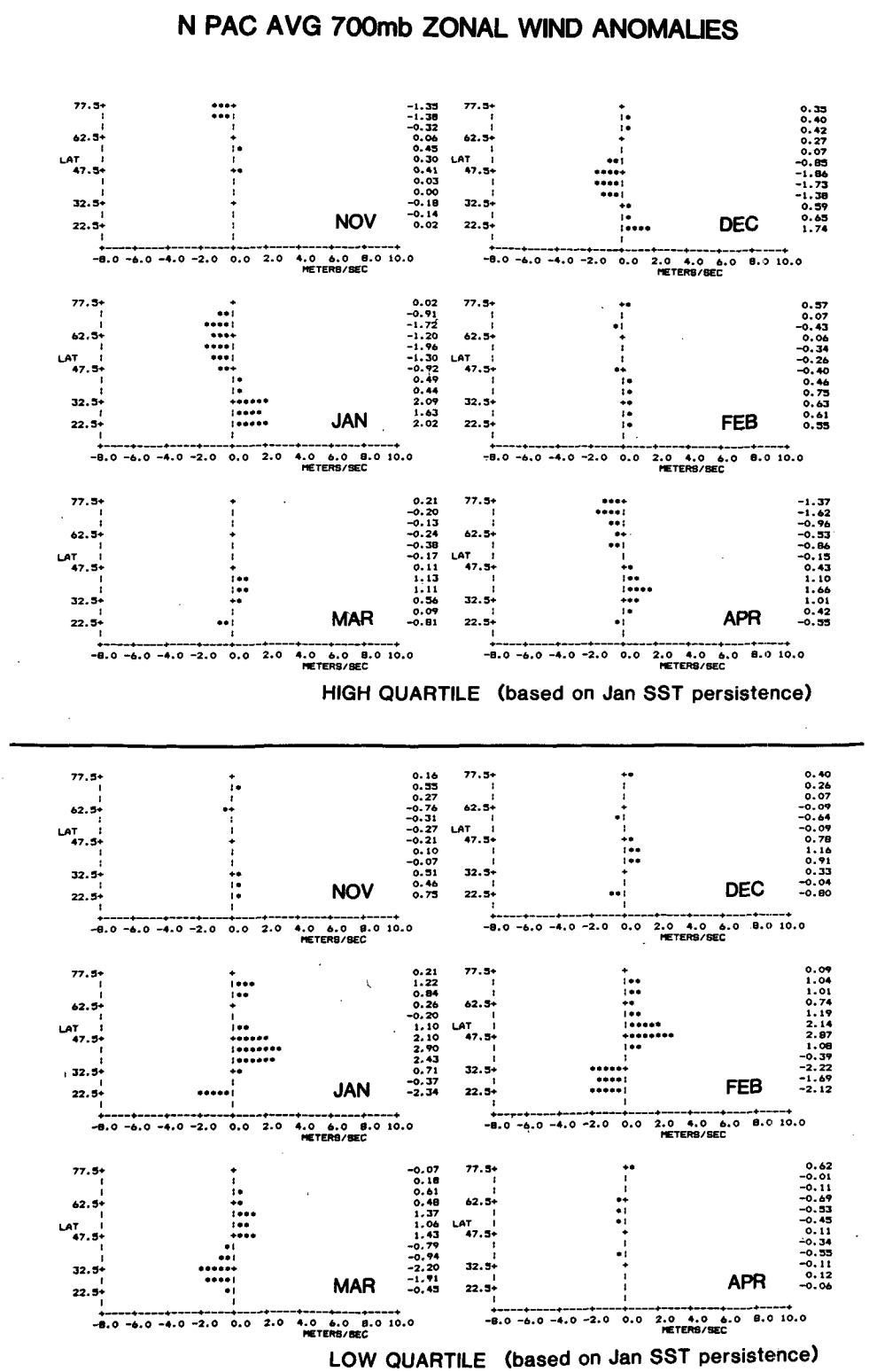

FIG. 12. Composite North Pacific 700 mb zonal wind anomalies (m s^{-1}) for indicated months for high (upper) and low (lower) quartile SST persistence cases. Composites consist of antecedent Novembers and Decembers, Januaries, and subsequent Februaries, Marches, and Aprils relative to high/low persistent January SST cases. Based on eight cases for each composite. Geotrophic winds calculated from 700 mb height averaged across North Pacific from 130°E to 110°W.

tence Januaries, are desirable to interpret results. The most obvious conclusion is that SST persistence from January to subsequent months is enhanced when there is an expanded (southerly displaced) westerly vortex, wherein westerly winds are stronger than normal over the subtropics (from 20°N to 35°N) and subnormal in temperate latitudes (35°N to 55°N). Previous studies, e.g., Namias (1965) suggested that this type of circulation is most persistent for several successive 5-day periods during winter, and the results here indicate that this holds for monthly time scales as well, since Fig. 12 shows that this general profile appears for the Decembers antecedent and Januaries subsequent to the high persistence Januaries in question. The statistical significance of these anomaly profiles can be judged by the standard deviation of the entire sample set of zonal wind anomalies, which ranges from about 1 to 3 m s^{-1} over all latitudes of these cool season months (shown in Fig. 13 for January). The distribution of the mean (or composite) of eight random, normally distributed

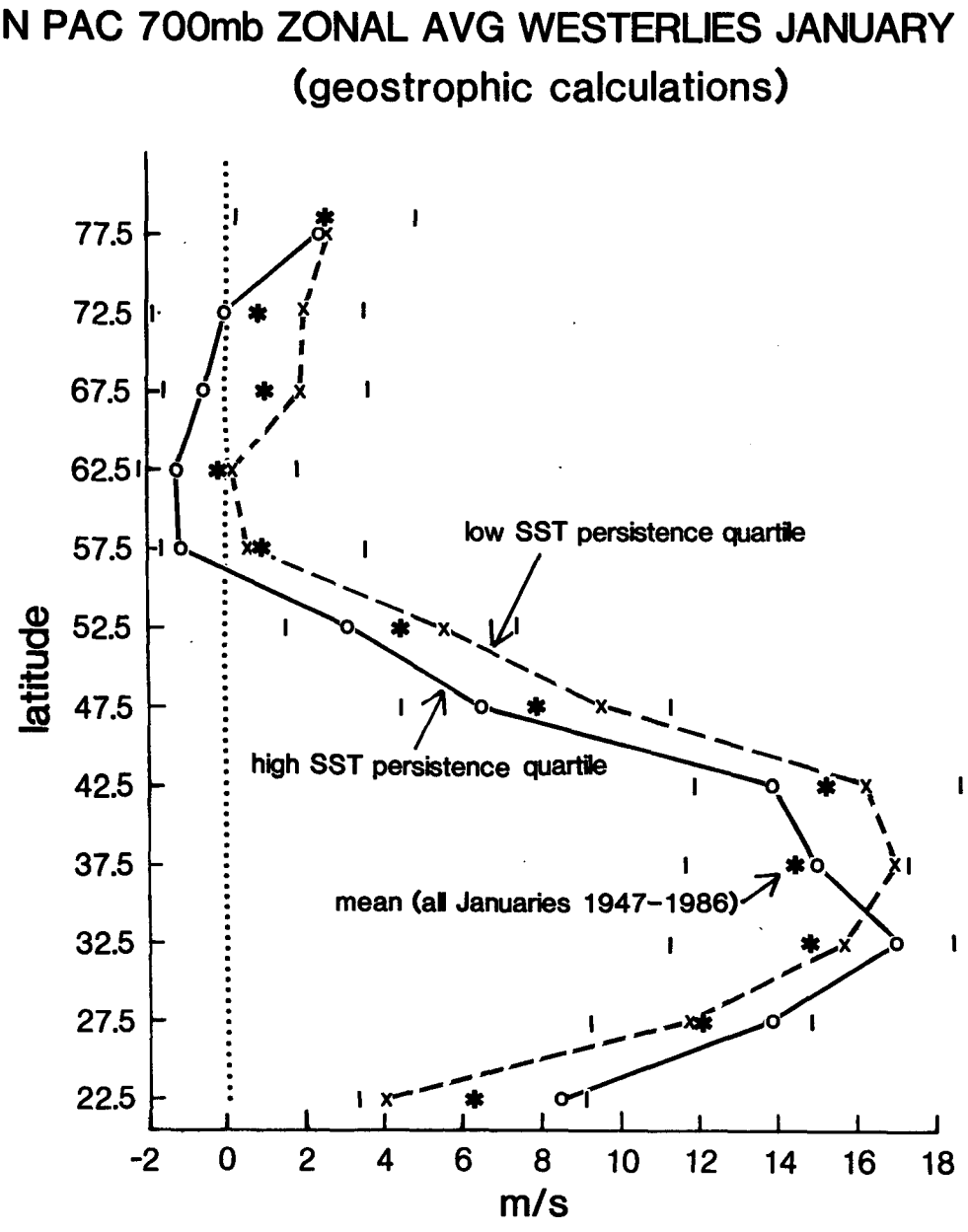

FIG. 13. Composite North Pacific 700 mb zonal wind (m s^{-1}) profiles for Januaries of high (solid line) and low (dashed line) quartile SST persistence cases. Long-term means indicated by asterisks; +/− standard deviations indicated by vertical bars. These zonal winds correspond to the January anomalies shown in Fig. 12.

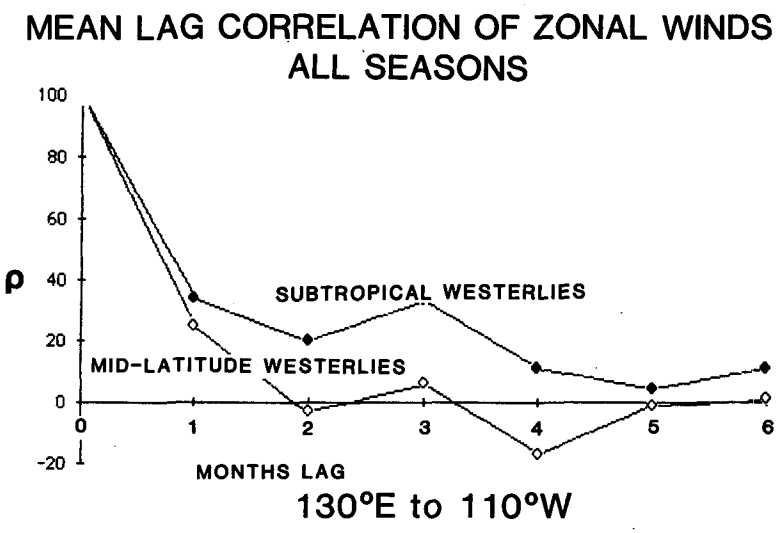

FIG. 14. Mean autocorrelations for North Pacific subtropical westerlies and midlatitude westerlies from initial month of January out to 6 months. Note consistently higher persistence of subtropical zonal winds over midlatitude winds.

variables would have a resultant standard deviation that is reduced by $1/\sqrt{8}$, yielding a maximum standard deviation of about 1 m s^{-1}. Since several of the composite anomaly features exceed 1 or even 2 m s^{-1}, these features appear to be statistically significant.

The composite zonal wind speed profiles corresponding to low persistence are much different from those for high persistence. During low persistence periods, zonal wind anomalies (Fig. 12, lower) are actually fairly strong, especially for January and the subsequent February and March, but the wind anomaly profiles are nearly opposite to the high persistence profiles, with enhanced westerlies in the *midlatitudes* (north of 32.5°N) and diminished westerlies in the subtropics. The mean wind speed composite profile for the low persistence Januaries is shown in Fig. 13. The penetration of the westerlies southward into the subtropics during the high SST persistence cases, and the contraction northward during low SST persistence episodes, are illustrated by the actual wind profiles.

Along with the differences between the *mean* zonal wind profiles corresponding to high and low persistence January SST cases, the *persistence* of the profiles was stronger for the high cases versus the low cases. The 1-month lag pattern correlation for December, January, and February 700 mb zonal wind anomalies was 0.44 for the high SST persistence cases and 0.28 for the low SST persistence cases. About five independent spatial samples in the zonal mean profiles and 24 independent time samples result in 120 samples, to yield a standard deviation for the correlation estimate of $1/(120-2)^{1/2}$, ~0.09. The difference between the two pattern correlation estimates (0.44–0.28) approaches twice the estimated sampling variation, and so it appears to be statistically significant.

We seem to have here a sort of high momentum atmospheric flywheel, which affects atmospheric and ocean wind pattern and SST pattern stability. When westerlies are enhanced in the subtropics, the 700 mb height tends toward the pattern in Fig. 6 and persists longer than when the westerlies are increased in midlatitudes and diminished in the subtropics. For the latter wind profile, the monthly anomaly pattern is more changeable, which is associated with the weaker SST persistence.

Other evidence shows the tenacity of expanded subtropical westerly circulations. When stratified in terms of subtropical westerlies and midlatitude westerlies, as shown in Fig. 14, lag correlations demonstrate that in the subtropics, persistence is substantially greater. In order to increase the confidence in this result, this figure is based on data for all seasons. It indicates once more the dominant influence of the expanded circumpolar vortex, and also confirms the well-known fact that atmospheric persistence is greater in low than in high latitudes (Landsberg et al. 1943; Namias 1954b).

It is interesting that the differences between persistence of zonal winds in the subtropics versus temperate latitudes exist even though these two wind systems are themselves strongly correlated (negatively), as shown in Table 4.

6. Long period swings in persistence of North Pacific SST patterns

The purpose of this section is to examine long-period (several-year) fluctuations in SST persistence. Some pronounced long period signals lasting years and decades are indicated in Fig. 15, which shows the persistence values for the 6 months following January, April,

TABLE 4. Contemporary correlation of 700 mb zonal wind over the North Pacific between the temperate latitude westerlies (35°N–55°N) and the subtropical westerlies (20°N–35°N).

J	F	M	A	M	J	J	A	S	O	N	D
−.46	−.52	−.56	−.49	−.54	−.50	−.45	−.53	−.54	−.46	−.30	−.58

July and October of each year (solid lines), their 5-yr running means (dotted lines), and their linear trend over the period of record (broken straight lines). Persistence was relatively strong from the mid-1950s to the mid-1960s but then weak from the mid-1960s until the mid-1970s, after which it again became stronger. In forecasting practice, long period persistence of SST patterns has frequently been observed, so the curves in Fig. 15 were not surprising, although the magnitude of the fluctuations was not expected. Indeed, some published studies have indicated such long-period trends in other climate variables (Namias 1952; Sheaffer and Reiter 1985). Assuming that these trends are real, they pose questions relating to understanding and possibly predicting climate in both air and sea involving periods of years—possibly the most important and economically valuable of all long-range forecasts.

In view of the association between high SST persistence and strengthened subtropical westerlies discussed above, the time series of zonal average subtropical westerlies is shown in the bottom plot of Fig. 15 for comparison with that of the SST persistence. Compared to the SST behavior, the North Pacific subtropical westerlies show a similar increase over time, and indeed, fluctuations within this record that match those of the SST persistence; e.g., the low values of the beginning of the record, high values in the late 1950s and early 1960s, and highs again in the late 1970s and early 1980s. This suggests a physical linkage to the SST persistence fluctuations.

Since strong persistence cases are associated with characteristic SST and atmospheric circulation anomaly patterns, it is of interest to further compare the persistence time series with some appropriate large-scale indices: the first EOF of North Pacific SST, the Pacific/North American (PNA) index by Horel and Wallace (1981), and the Southern Oscillation Index as tabulated in the NOAA Climate Diagnostics Bulletin. These are shown as 5-yr running means in the series of plots in Fig. 16. The composite SST anomaly during

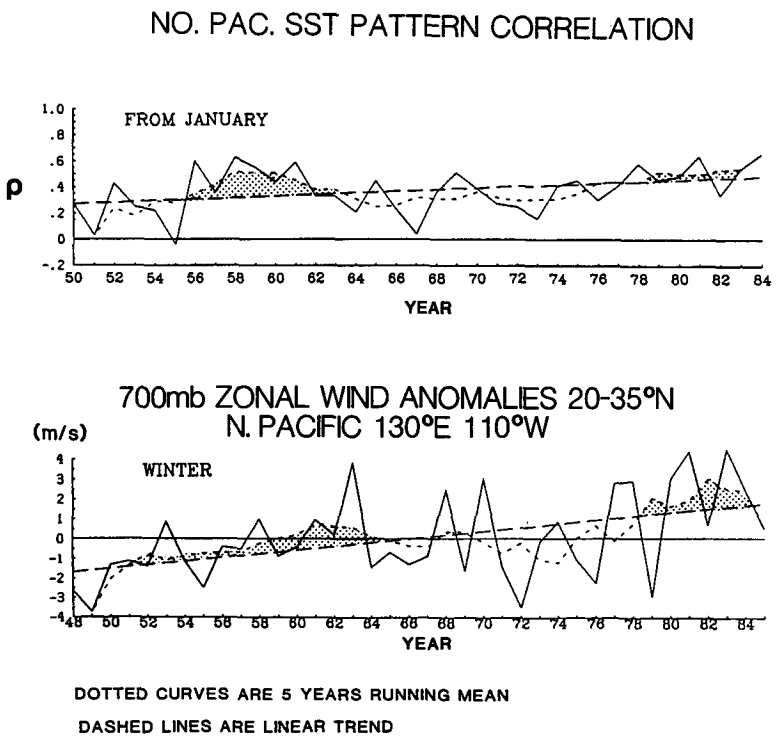

FIG. 15. North Pacific January SST persistence index (upper) and North Pacific winter 700 mb zonal wind in subtropics (lower) 1950–84. Short dashed curve is 5-yr running mean, and the broken straight sloping line is linear trend.

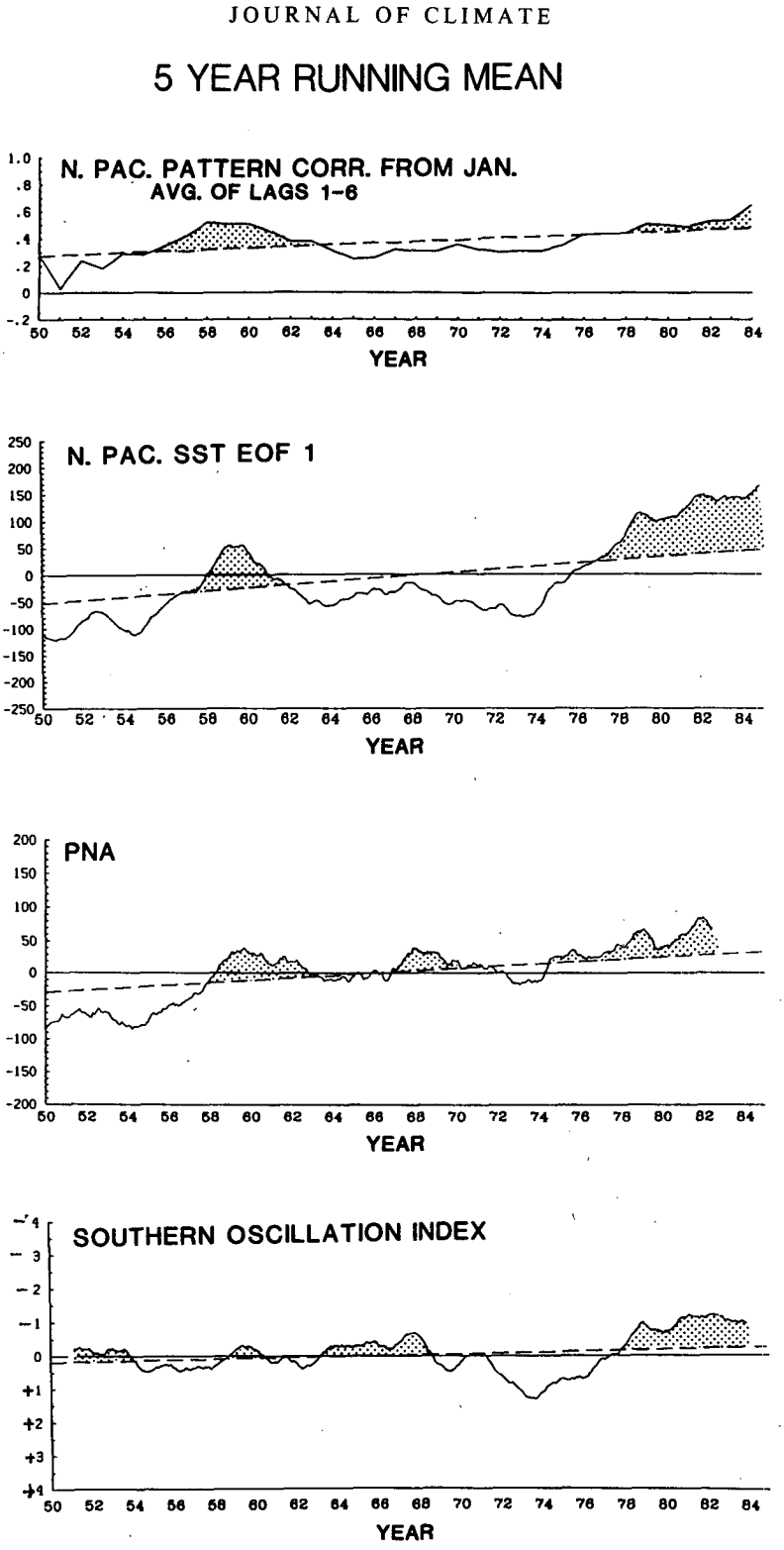

FIG. 16. Five-year running mean of January SST persistence index, amplitude of North Pacific SST EOF 1, Pacific/North American (PNA) index from 700 mb height (after Horel and Wallace 1981), and Southern Oscillation Index (from NOAA Climate Analysis Center's Climate Diagnostic Bulletin, 1986). Southern Oscillation Index is plotted with negative values up for easier comparison with other time series. Broken line is the linear trend of each variable.

high persistence cases in section 3 suggests that SST persistence is correlated with the amplitude of North Pacific SST EOF 1. Figure 16 (second from top) demonstrates that episodes having a high positive phase of EOF 1 are indeed associated with greater persistence, as anticipated. The running mean of the PNA index (Fig. 16, third from top) shows a strong atmospheric connection to SST EOF 1, the SST persistence, and to the 700 mb zonal average westerlies. Besides the year-to-decade-scale fluctuations, there is a significant upward linear trend in the PNA index; it's rise over this period is consistent with the upward trend in both SST EOF 1 and SST persistence. Barnston and Livezey (1987) have shown that the PNA pattern exhibits significant persistence during winter months. Also, the atmospheric circulation over North America and adjacent oceanic sectors of the Northern Hemisphere tends to be more persistent during ENSO episodes (Namias 1986). Moreover, North Pacific SST fluctuations also seem to be related to the Southern Oscillation Index (SOI). (See Fig. 16, bottom, plotted with negative values upward for easier comparison.) In the atmosphere, the relationship between ENSO phenomena and a deepened central North Pacific low have been reported by a number of authors, e.g., Bjerknes (1966), Horel and Wallace (1981), Namias (1985), and Dickson and Livezey (1984). In the ocean, it is well established that ENSO phenomena are associated with negative SST anomalies in the central North Pacific (Wagner 1984; Oort and Pan 1985). In view of these observations, it is not surprising to find a correspondence between SST persistence and associated large-scale ENSO-related variations, although not as strikingly as with the other two indices. The SOI shows negative excursions correlated with high persistence North Pacific SST and associated atmospheric behavior from 1958 to 1960, in the middle to late 1960s, and from the late 1970s through 1983. The SOI also displays a decreasing linear trend that is consistent with the increases in the other indices.

The trend toward more persistent SST anomalies during the last decade of this record is remarkable. Independent evidence supporting the composites of the previous sections is provided from SST and 700 mb height data available since 1982, beyond the record used in the anomaly composites. Four of the five winters (1983, 1984, 1986 and 1987) exhibited strong persistence of *both* SST and 700 mb height, as shown by the pattern correlations from January (Table 5). The pattern of SST and 700 mb anomalies averaged over these four Januarys, shown in Fig. 17, has a large amplitude because of the similarity of the patterns for the individual years. This pattern resembles the high persistence composites (Figs. 4 and 6), although the 1983–87 patterns are shifted westward from the composite by about 10° longitude.

Can we believe the strong trend of the SST pattern and its persistence over the last four decades? If there were no corroborating atmospheric evidence, it would be possible to dismiss this as a data problem, perhaps an instrumental artifact. However, the atmospheric evidence suggests that the qualitative nature of the trend in the SST field is a real feature. Decadal scale changes in 700 mb height anomalies (Douglas et al. 1982) and sea level pressure anomalies (Venrick et al. 1987) appear consistent with the SST: the strongest increased zonal winds have occurred over the region of strongest negative SST anomalies in the central North Pacific, while the positive 700 mb height anomalies and/or increased southerly flow has coincided with positive SST anomalies in the far eastern North Pacific. Other studies, e.g., Davis (1976) and Graham (1986), show that these SST and atmospheric anomaly pattern relationships hold up well statistically. Along with the similarity of the pattern of the post-1982 SST and 700 mb height anomalies to their composites, it follows that the 700 mb geostrophic zonal wind anomalies are consistent with the zonal wind composites from the larger dataset. They also show increased westerlies in the lower latitudes (south of about 40°N) and decreased westerlies in higher midlatitudes (north of about 45°N).

7. Summary and conclusions

About four decades of monthly SST and 700 mb height data have been used to explore the persistence of large-scale SST anomalies in the North Pacific and how it relates to atmospheric circulation. On averaging, North Pacific SST anomaly patterns have lifetimes of 3–5 months and have sizable lag correlations out to 12 months; these lag correlations are greater than expected by a first-order Markov process. The persistence undergoes an annual cycle—the strongest memory of the system is in winter and spring, when the mixed layer is deepest. For this reason, most of the analyses were focused on SST persistence calculated during winter. Using January SST as the leading variable in the lagged pattern correlation, the average over lags of 1–6 months was used as an index of persistence. The cases comprising the high and low quartiles of the SST persistence (eight cases each) for the 1950–82 period were compared to study the macroscale SST patterns and corresponding atmospheric circulation associated with persistent and with antipersistent episodes.

The results indicate that SST persistence patterns over the North Pacific are not random, but have characteristics that are related to the nature and form of the initial monthly or seasonal SST pattern. In turn, these are related to the initial atmospheric flow patterns and their associated wind speed profiles. The SST pattern with strongest persistence features negative anomalies in the east-central North Pacific and positive anomalies along the West Coast. The high persistence 700 mb anomaly pattern had a strong negative anomaly centered off the West Coast at about 40°N, 155°W, with positive anomalies over much of North America,

TABLE 5. Pattern correlation by initial month for November 1982–April 1987 at lags of 1–6 months and averaged over lags 1–3 and 1–6 months. Anomalies based on 1947–66 long-term mean.

	SST Lag (months)									700 mb Lag (months)							
Initial mo	1	2	3	4	5	6	1–3	1–6	Initial mo	1	2	3	4	5	6	1–3	1–6
1982 10	0.33	0.40	0.36	0.34	0.48	0.34	0.36	0.38	1982 10	−0.17	−0.61	−0.35	−0.39	−0.36	−0.23	−0.38	−0.35
1982 11	0.34	0.36	0.27	0.33	0.23	0.17	0.32	0.28	1982 11	0.52	0.31	0.33	0.40	0.65	0.24	0.39	0.41
1982 12	0.57	0.51	0.40	0.39	0.40	0.26	0.49	0.42	1982 12	0.62	0.66	0.59	0.41	0.48	0.26	0.62	0.50
1983 1	0.71	0.69	0.62	0.55	0.41	0.33	0.67	0.55	1983 1	0.90	0.89	−0.06	0.17	0.48	0.30	0.58	0.45
1983 2	0.81	0.80	0.78	0.61	0.54	0.73	0.80	0.71	1983 2	0.90	0.03	0.19	0.47	0.33	−0.13	0.37	0.30
1983 3	0.88	0.79	0.64	0.56	0.70	0.45	0.77	0.67	1983 3	0.02	0.19	0.54	0.32	−0.17	−0.24	0.25	0.11
1983 4	0.84	0.62	0.50	0.66	0.45	0.28	0.65	0.56	1983 4	0.16	−0.09	0.16	−0.02	−0.12	0.24	0.08	0.05
1983 10	0.77	0.47	0.38	0.37	0.24	0.34	0.54	0.43	1983 10	−0.23	0.18	−0.37	−0.09	−0.20	−0.42	−0.14	−0.19
1983 11	0.71	0.54	0.55	0.48	0.52	0.47	0.60	0.55	1983 11	0.03	0.23	0.56	0.65	0.76	0.46	0.27	0.45
1983 12	0.74	0.76	0.75	0.70	0.65	0.55	0.75	0.69	1983 12	0.11	−0.44	0.29	−0.24	−0.12	−0.38	−0.01	−0.13
1984 1	0.88	0.87	0.70	0.62	0.51	0.45	0.82	0.67	1984 1	0.37	0.71	0.41	0.32	−0.26	0.15	0.50	0.28
1984 2	0.88	0.76	0.70	0.62	0.52	0.53	0.78	0.67	1984 2	0.47	0.66	0.49	0.19	0.10	−0.03	0.54	0.31
1984 3	0.81	0.76	0.62	0.56	0.55	0.56	0.73	0.64	1984 3	0.49	0.28	0.05	−0.28	−0.20	−0.04	0.27	0.05
1984 4	0.83	0.68	0.50	0.50	0.56	0.59	0.67	0.61	1984 4	0.72	0.30	0.03	−0.15	−0.07	0.00	0.35	0.14
1984 10	0.50	0.68	0.61	0.57	0.37	0.25	0.60	0.50	1984 10	0.01	0.28	−0.06	0.26	−0.35	−0.43	0.08	−0.05
1984 11	0.57	0.39	0.28	0.33	0.23	0.06	0.41	0.31	1984 11	−0.12	−0.08	−0.48	0.53	−0.14	0.45	−0.23	0.03
1984 12	0.80	0.70	0.61	0.34	0.25	0.17	0.70	0.48	1984 12	−0.37	0.24	−0.04	−0.43	0.27	−0.40	−0.06	−0.12
1985 1	0.85	0.65	0.35	0.23	0.15	0.42	0.62	0.44	1985 1	−0.40	−0.24	−0.29	−0.41	−0.11	0.26	−0.31	−0.20
1985 2	0.66	0.36	0.27	0.11	0.36	0.21	0.43	0.33	1985 2	−0.25	0.35	−0.08	−0.05	−0.14	0.18	0.01	0.00
1985 3	0.64	0.44	0.30	0.40	0.29	0.24	0.46	0.38	1985 3	0.37	0.51	0.22	−0.46	0.12	−0.16	0.37	0.10
1985 4	0.55	0.54	0.34	0.33	0.16	0.27	0.48	0.37	1985 4	0.14	0.43	−0.25	0.05	−0.46	−0.09	0.11	−0.03
1985 10	0.75	0.66	0.53	0.41	0.34	0.42	0.65	0.52	1985 10	0.50	−0.54	−0.67	−0.65	−0.68	0.67	−0.24	−0.23
1985 11	0.74	0.38	0.25	0.18	0.23	0.35	0.46	0.36	1985 11	−0.06	−0.70	−0.07	−0.50	0.02	−0.09	−0.28	−0.23
1985 12	0.66	0.57	0.46	0.38	0.41	0.24	0.56	0.45	1985 12	0.42	0.54	0.42	−0.55	−0.64	0.19	0.46	0.06
1986 1	0.85	0.81	0.76	0.65	0.54	0.53	0.81	0.69	1986 1	0.59	0.85	−0.38	0.11	0.54	−0.28	0.35	0.24
1986 2	0.89	0.83	0.73	0.68	0.60	0.48	0.82	0.70	1986 2	0.81	−0.56	−0.16	−0.01	0.28	0.32	0.03	0.11
1986 3	0.84	0.78	0.73	0.59	0.48	0.55	0.78	0.66	1986 3	−0.39	0.08	0.26	0.05	0.40	−0.42	−0.02	0.00
1986 4	0.79	0.65	0.61	0.50	0.51	0.58	0.68	0.61	1986 4	0.42	−0.23	0.09	−0.14	−0.01	−0.41	0.09	−0.05
1986 10	0.87	0.80	0.66	0.53	0.50	0.34	0.78	0.62	1986 10	0.32	0.49	0.19	0.57	0.69	0.12	0.33	0.40
1986 11	0.81	0.73	0.62	0.58	0.46	0.36	0.72	0.59	1986 11	−0.05	−0.17	−0.18	−0.09	−0.16	−0.25	−0.13	−0.15
1986 12	0.83	0.75	0.72	0.61	0.52	−0.03	0.77	0.57	1986 12	0.83	0.82	0.74	0.61	−0.27	0.19	0.80	0.49
1987 1	0.86	0.82	0.69	0.59	0.10	0.57	0.79	0.61	1987 1	0.71	0.67	0.87	0.10	0.53	0.15	0.75	0.50
1987 2	0.96	0.79	0.70	0.24	0.65	0.59	0.82	0.66	1987 2	0.90	0.56	−0.09	0.15	0.41	0.31	0.46	0.37
1987 3	0.76	0.72	0.28	0.61	0.51	0.50	0.59	0.56	1987 3	0.55	−0.11	0.02	0.53	0.47	−0.21	0.15	0.21
1987 4	0.75	0.31	0.59	0.55	0.51	0.48	0.55	0.53	1987 4	0.32	0.62	−0.03	−0.19	0.19	0.14	0.30	0.18

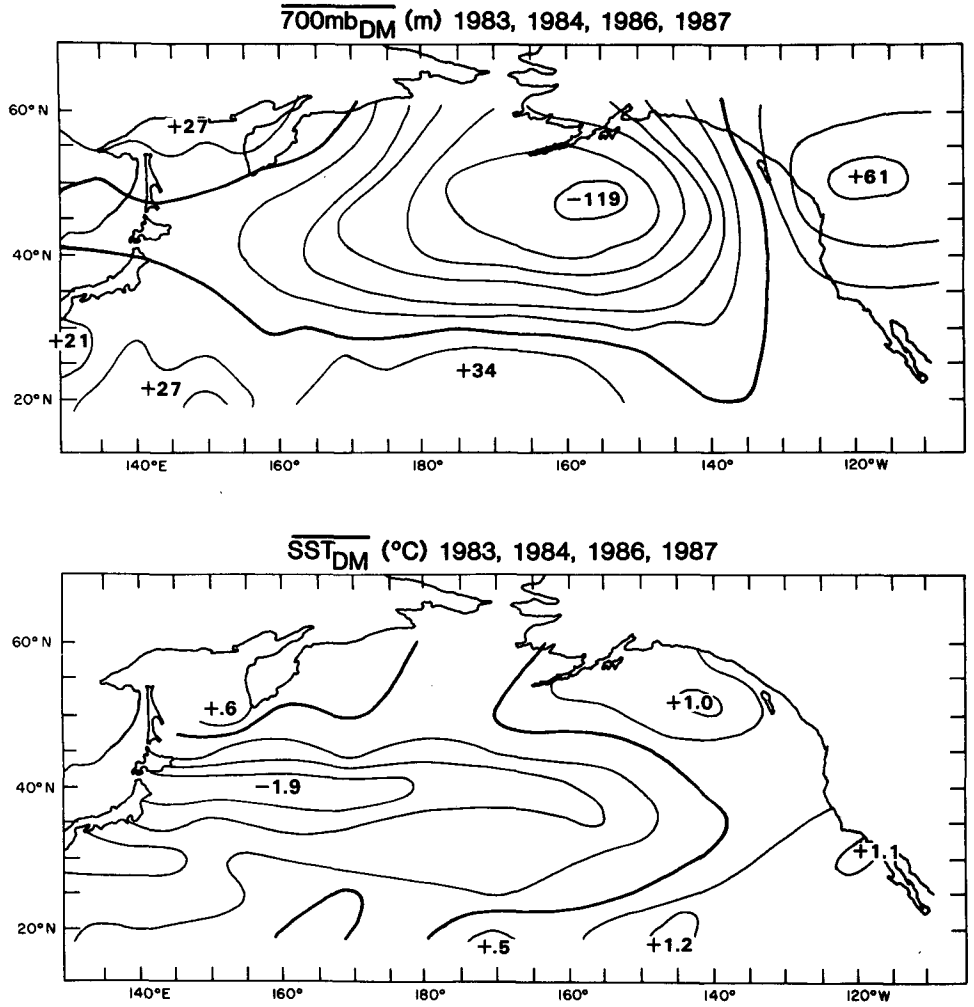

FIG. 17. Average 700 mb height anomaly (m) (top) and SST anomaly (°C) (bottom) for four recent Januarys: 1983, 1984, 1986, and 1987.

a pattern similar to the frequent atmospheric mode, the PNA pattern.

Another contrast between atmospheric circulations associated with this high and low SST persistence is provided by averaging the midtropospheric westerly winds across the North Pacific. The high persistence profile had strengthened in the subtropics but had weakened zonal westerlies in midlatitudes. The 700 mb zonal wind anomaly profile corresponding to high persistence January SST cases was nearly opposite to that for low persistence. Thus, the SST persistence is often strongest subsequent to Januarys when the atmospheric circulation is initially composed of an expanded circumpolar vortex—a result also found for the atmosphere over North America. For both the January SST high and the low persistence composites, these anomaly profiles appeared in three of the winter months adjacent to the given January. The high persistence situation may be related to the fact that subtropical atmospheric anomalies have longer lifetimes than those in midlatitudes; this is true for both the pattern of 700 mb height and the zonal average winds. This latitudinal variation in persistence of the zonal wind shows up in lag correlations over the entire sample as well as for individual seasons. While this phenomenon is probably related to large-scale blocking, the precise mechanisms are poorly understood. It is noteworthy that studies of regional blocking suggest that persistence of blocks is greater than that of other modes of circulation (Øklund and Lejenas 1987).

The high persistence SST patterns were associated with midtropospheric wind systems that were also persistent. The 700 mb height anomaly patterns corresponding to high January SST persistence cases showed strong patterns that were persistent from December through February, while those for the low persistence cases changed radically from January to February. To a certain extent, SST behaves like a low pass filter of

atmospheric forcing, since the characteristic high January SST persistence 700 mb pattern appeared in the preceding month of December—i.e., the strong SST pattern had at least a month to develop. The resultant SST pattern was then associated with a stable atmospheric pattern that continued through February. Although a strong recurring atmospheric pattern appears to be required to set it up, evidence does not dispel the sea-to-air feedback possibility. An important question remains: To what degree does the persistent SST anomaly pattern feed back to the atmospheric circulation?

When persistence values were graphed by season and year, a striking low frequency 5-yr overlapping mean curve emerged, suggesting a "cycle" of a decade or more. Furthermore, a long period upward trend in persistence appeared over the years 1950 to the mid-1980s. Over this period, the North Pacific SST field has shown more persistence when there is high amplitude meridional wind anomalies and the positive phase of the PNA pattern is strong (low pressure in central North Pacific, high pressure in the West). In turn, this has tended to occur during ENSO episodes. The corresponding phase of SST EOF 1, with negative anomalies in the central North Pacific and positive anomalies along the West Coast, is well related to the PNA, which has occurred frequently in the last decade. High spells of SST persistence occurred in the late 1950s and also in the late 1970s and early 1980s, corresponding to high PNA episodes and, to some extent, pronounced ENSO events.

The mechanism driving the long-period phenomena remains unexplained, but we note that there has been a corresponding long-term increase in the midtropospheric subtropical westerlies and in the frequency of El Niño episodes. Also, some correlations of the SST persistence with sunspot activity imply the possibility of a weak relationship for fall and winter periods but not for other seasons. It is quite clear that the low-frequency fluctuations observed in the Pacific have large coherent spatial patterns. These patterns probably have broad-ranging teleconnections and associated effects. Downstream from the North Pacific basin, it has been shown that decadal scale changes in the North Pacific SST and 700 mb height are related to variability at the surface and aloft over North America (Douglas et al. 1982). Bjerknes (1962) noted similar ocean temperature-atmosphere circulation changes in the North Atlantic sector over earlier decades. An investigation of biological activity in the upper ocean in the central North Pacific (Venrick et al. 1987) suggests a long-term increase in chlorophyl concentration, which apparently is associated with the deeper central North Pacific winter low pressure center and cooler SST during the last decade. If such variability is rooted in the tropics, it probably has global-scale links. For example, recent studies by Ropelewski and Halpert (1987) and Bradley et al. (1987) illustrate the spatially extensive connections of shorter term fluctuations of ENSO with an array of global and regional scale temperature and precipitation patterns.

The importance of these long period variations cannot be overestimated, since their understanding carries with it the hope of predicting economically important climate variations involving repetition of abnormal weather over spells of years.

Acknowledgments. Our thanks to John Roads and Huug Van den Dool for comments on the manuscript, Mary Ray for word processing, and Marguerette Schultz for illustration. The work was supported by the National Science Foundation under Grant ATM-8407891 and by the National Climate Program Office under Grant NA81AA-D-00054. Part of the support for Daniel R. Cayan was provided by the State of California Department of Boating and Waterways. Special thanks are due Dr. Chao of the National Research Center for Marine Environment Forecast, Beijing, China, and Dr. William Sprigg of NOAA for providing partial funding for Ms. Xiaojun Yuan.

REFERENCES

Barnston, A. G., and R. E. Livezey, 1987: Classification, seasonality and persistence of low-frequency atmospheric circulation patterns. *Mon. Wea. Rev.*, **115**, 1083–1126.

Bjerknes, J., 1962: Synoptic survey of the interaction of sea and atmosphere in the North Atlantic. Geofysiske Publikasjoner, *Geophysica Norvegica*, **24**(3), the Vilhelm Bjerknes Centenary Volume, 115–145.

——, 1966: A possible response of the atmospheric Hadley circulation to anomalies of ocean temperature. *Tellus*, **18**, 820–829.

Bradley, R. S., H. F. Diaz, G. N. Kiladis and J. K. Eischeid, 1987: ENSO signal in continental temperature and precipitation records. *Nature*, **327**, 497–501.

Davis, R., 1976: Predictability of sea surface temperature and sea level pressure anomalies over the North Pacific Ocean. *J. Phys. Oceanogr.*, **6**(3), 249–266.

——, 1978: Predictability of sea level pressure anomalies over the North Pacific Ocean. *J. Phys. Oceanogr.*, **8**, 233–246.

Dickson, R. R., and R. E. Livezey, 1984: On the contribution of major warming episodes in the tropical East Pacific to a useful prognostic relationship based on the Southern Oscillation. *J. Climat. Appl. Meteor.*, **23**, 194–200.

Douglas, A. V., D. R. Cayan and J. Namias, 1982: Large-scale changes in North Pacific and North American weather patterns in recent decades. *Mon. Wea. Rev.*, **110**, 1851–1862.

Frankignoul, C., 1985: Sea surface temperature anomalies, planetary waves, and air–sea feedback in the middle latitudes. *Rev. Geophys.*, **23**, 357–390.

Graham, N. E., 1986: Statistical models of Pacific Ocean sea surface temperatures. Ph.D. thesis, University of California, Santa Barbara.

Harnack, R. P., and A. J. Broccoli, 1979: Associations between sea surface temperature gradient and overlying mid-tropospheric circulation in the North Pacific region. *J. Phys. Oceanogr.*, **9**, 1232–1242.

Horel, J. D., 1985: Persistence of the 500 mb height field during Northern Hemisphere winter. *Mon. Wea. Rev.*, **113**, 2030–2042.

——, and J. M. Wallace, 1981: Planetary-scale atmospheric phenomena associated with the Southern Oscillation. *Mon. Wea. Rev.*, **109**, 813–829.

Klein, W. H., 1985: Space and time variations in specifying monthly

mean surface temperature from the 700 mb height field. *Mon. Wea. Rev.*, **113**, 277–290.

Landsberg, H., M. C. George and F. W. Appel, 1943: Studies on pressure, temperature and precipitation persistence. A series of unpublished reports by the military climatology project, University of Chicago.

Meehl, G. A., 1982: Characteristics of surface current flow inferred from a global ocean current dataset. *J. Phys. Oceanogr.*, **12**(6), 538–555.

Mo, K. C., and M. Ghil, 1987. Statistics and dynamics of persistent anomalies. *J. Atmos. Sci.*, **44**, 877–901.

Namias, J., 1952: The annual course of month-to-month persistence in climatic anomalies. *Bull. Amer. Meteor. Soc.*, **33**(7), 279–285.

——, 1953: Thirty-day forecasting: a review of a ten-year experiment. *Meteorological Monographs*, **2**(6).

——, 1954a: Quasi-periodic cyclogenesis in relation to the general circulation. *Tellus*, **6**, 8–22.

——, 1954b: Further aspects of month-to-month persistence. *Bull. Amer. Meteor. Soc.*, **35**, 112–117.

——, 1965: Stability of an expanded circumpolar vortex. *J. Atmos. Sci.*, **22**, 728–729.

——, 1966: A weekly periodicity in eastern U.S. precipitation and its relation to hemispheric circulation. *Tellus*, **18**, 731–744.

——, 1970: Macroscale variations in sea surface temperatures in the North Pacific. *J. Geo. Res.*, **75**(3), 565–582.

——, 1972: Large-scale and long-term fluctuations in some atmospheric and oceanic variables. *Nobel Symposium*, **20**, 27–48.

——, 1975: Stabilization of atmosphere circulation patterns by sea surface temperature. *J. Mar. Res.*, **33** supplement, 53–60.

——, 1978: Persistence of U.S. seasonal temperatures up to one year. *Mon. Wea. Rev.*, **106**, 1558–1567.

——, 1979: Northern Hemisphere seasonal 700 mb height and anomaly charts, 1947–1979, and associated North Pacific sea surface temperature anomalies. CalCOFI Atlas No. 27. A. Fleminger, Ed. Scripps Institution of Oceanography, 275 pp.

——, 1981: Teleconnections of 700 mb height anomalies for the Northern Hemisphere. CalCOFI Atlas No. 29. A. Fleminger, Ed. Scripps Institution of Oceanography, 265 pp.

——, 1983: Short period climatic variations: Collected works of J. Namias, 1975 through 1982, Vol. III, 393 pp.

——, 1985: New evidence for relationships between North Pacific atmospheric circulation and El Niño. *Trop. Ocean-Atmos. Newslett.*, No. 30, 2–3.

——, 1986: Persistence of flow patterns over North America and adjacent ocean section. *Mon. Wea. Rev.*, **114**(7), 1368–1383.

——, and R. M. Born, 1970: Temporal coherence in North Pacific sea-surface temperature patterns. *J. Geophys. Res.*, **75**, 5952–5955.

——, and ——, 1972: Empirical techniques applied to large-scale and long-period air-sea interactions, a preliminary report. *SIO Ref. 72-1*, 47 pp.

NOAA/National Weather Service, 1986: Climate Diagnostics Bulletin, Global Analyses and Indices, No. 86/4. V. E. Kousky, Ed. 53 pp.

Øklund, H., and H. Lejenas, 1987: Blocking and persistence. *Tellus*, **39A**, 33–38.

Oort, A. H., and Y-H. Pan, 1985: Diagnosis to historical ENSO events. *WMO Long-Range Forecasting Research Report Series*, **1**, No. 6, 249–258. Proceedings of the First WMO Workshop combined with NOAA's Tenth Annual Climate Diagnostics Workshop, College Park, MD 20742.

Palmer, T. N., 1987: Medium and extended range predictability, stability of the PNA mode, and atmospheric response to sea surface temperature anomalies. Submitted to *Mon. Wea. Rev.*

Panofsky, H. A., and G. W. Brier, 1958: Some Applications of Statistics to Meteorology. *College of Mineral Industries, The Pennsylvania State University*, University Park, PA 16802, 224 pp.

Rex, D. F., 1950: Blocking action in the middle troposphere and its effect upon regional climate. Part II: The climatology of blocking action. *Tellus*, **2**, 275–301.

Roads, J. O., and T. Barnett, 1984: Forecasts of the 500 mb height using a dynamically oriented statistical model. *Mon. Wea. Rev.*, **112**, 1354–1369.

Ropelewski, C. F., and M. S. Halpert, 1987: Global and regional-scale precipitation patterns associated with the El Niño/Southern Oscillation. *Mon. Wea. Rev.*, **115**, 1606–1626.

Sheaffer, J. D., and E. R. Reiter, 1985: Influence of Pacific sea surface temperatures on seasonal persistence over the western plateau of the United States. *Arch. Meteor. Geophys. Bioklim.*, Ser. **A34**, 111–130.

Van den Dool, H. M., 1983: A possible explanation of the observed persistence of monthly mean circulation anomalies. *Mon. Wea. Rev.*, **111**, 539–544.

——, and T. M. Chervin, 1986: A comparison of month-to-month persistence of anomalies in a general circulation model and in the earth's atmosphere. *J. Atmos. Sci.*, **43**, 1454–1466.

——, W. H. Klein and J. E. Walsh, 1986: The geographical distribution and seasonality of persistence in monthly mean air temperatures over the United States. *Mon. Wea. Rev.*, **114**, 546–560.

Venrick, E. L., J. A. McGowan, D. R. Cayan and T. L. Hayward, 1987: Climate and chlorophyll a: Long-term trends in the central North Pacific Ocean. *Science*, **238**, 70–72.

Wagner, A. J., 1984: Possible midlatitude atmospheric generation of anomalously warm surface waters in the Gulf of Alaska from autumn 1982 to spring 1983. *Trop. Ocean-Atmos. Newslett.*, No. 26, 15–16.